SE-SSL-1678

SE-SSL-1678

Final Report

ANALYTICAL STUDY OF SPACECRAFT DEPOSITION CONTAMINATION BY INTERNAL REFLECTION SPECTROSCOPY

December 1972

CASE FILE COPY

BROWN ENGINEERING

Research Park • Huntsville, Alabama 35807

Page Intentionally Left Blank

FINAL REPORT
SE-SSL-1678

ANALYTICAL STUDY OF SPACECRAFT DEPOSITION
CONTAMINATION BY INTERNAL REFLECTION SPECTROSCOPY

By

T. Mookherji

December 1972

Prepared For

NUCLEAR AND PLASMA PHYSICS DIVISION
SPACE SCIENCES LABORATORY
GEORGE C. MARSHALL SPACE FLIGHT CENTER

Contract No. NAS8-28533

Prepared By

SCIENCE AND ENGINEERING
TELEDYNE BROWN ENGINEERING
HUNTSVILLE, ALABAMA

ABSTRACT

Infrared absorption spectra of ten individual contaminant materials and four binary mixtures of these have been studied using the Internal Reflection Spectroscopy technique. The effect of ultraviolet radiation on these contaminants has also been studied. It has been observed that all siloxanes, silanes, and esters are drastically affected by ultraviolet irradiation. In most cases polymerization and tar formation results.

Approved By:

N. E. Chatterton, Ph. D.
Manager
Research Laboratories

TABLE OF CONTENTS

LIST OF ILLUSTRATIONS

LIST OF ILLUSTRATIONS - Concluded

INTRODUCTION

The contamination of spacecraft due to material outgassing has been recognized as a problem from the beginning of the space program. The specific dangers arising from the presence of contaminants are

- The development of localized atmosphere consisting of cabin leakage products, fuel cell wastes, etc.

- The deposition and adhesion of both particulate matter and gaseous condensates upon sensitive optical, thermal control, and solar cell surfaces.

- The interference, through light absorption and scattering, with signal reception.

Deposits on critical optical, thermal control and solar cell surfaces of Skylab, LST, and other space programs could adversely affect the very basis of the different experiments.

Furthermore, ultraviolet photons and solar protons and electrons possess sufficient energy to produce photochemical reactions in the contaminant and cause fission of chemical bonds, polymerization and cross-linking of a very complex nature.

In situ and other types of cleaning of the contaminated surfaces are proposed to overcome the contamination problem. To locate and control the sources of contamination and to devise the appropriate cleaning technique it is necessary to identify the contaminant materials and to find the changes occurring in them due to solar radiation.

The present study is concerned with the identification of the contaminant materials and the observation of the effects of ultraviolet radiation on them. Infrared Internal Reflection Spectroscopy (IRS) technique is used for this purpose.

1

Spectra of ten monocomponent systems and four binary mixtures are presented both before and after irradiation with ultraviolet light. The results are discussed in terms of the identification of the different absorption bands and the effect of ultraviolet irradiation on them. Recommendations are made about future development of this approach.

An appendix is included to show the ultimate sensitivity of the present IRS technique for identification of very small amounts of contaminant material.

PRINCIPLES OF INTERNAL REFLECTION SPECTROSCOPY

The optical properties of absorbing media may be described quantitatively by the complex refractive index, $\widetilde{N} = n + ik$, where n, the real part of the refractive index, is defined as the ratio of the velocity of light in vacuum (c) to the phase velocity (v) in the dielectric of a plane electromagnetic wave having constant amplitude along a wave front,

$$n = c/v . \tag{1}$$

The imaginary part of the complex refractive index, k, often called the extinction coefficient, describes the damping of the wave as it traverses the absorbing medium, and is defined by the relation

$$E = E_0 \exp \left(- \frac{2\pi \, kz}{\lambda} \right) \tag{2}$$

where

z - coordinate in the direction of propagation

E_0 - amplitude of the electromagnetic wave at $z = 0$

E - amplitude at z

λ - wavelength of the electromagnetic wave in vacuum.

The theory of reflection and transmission of light by thin films has been discussed in many texts. Expressions for the reflectance (R) at a given wavelength are obtained by the application of boundary conditions to Maxwell's equations for a plane electromagnetic wave incident on the boundary between two media.

When a plane wave falls onto a boundary between two homogeneous media of different optical properties, it is split into two

waves: a transmitted wave proceeding into the second medium and a reflected wave propagated back into the first medium. The existence of these two waves can be demonstrated from the boundary conditions, since it is easily seen that these conditions cannot be satisfied without postulating both the transmitted and the reflected wave. The transmitted beam is refracted according to Snell's law:

$$n_1 \sin \theta = n_2 \sin \phi \tag{3}$$

where

n_1 - the refractive index in medium 1

n_2 - the refractive index in medium 2

θ - the angle of incidence in medium 1

ϕ - the angle of refraction in medium 2.

For the reflected beam, the angle of reflection is equal to the angle of incidence. The reflected amplitudes for unit incident amplitudes for light with the electric field vector perpendicular and parallel to the plane of incidence, respectively, are given by Fresnel's equations,

$$R_{\perp} = \frac{n_1 \cos \theta - n_2 \cos \phi}{n_1 \cos \theta + n_2 \cos \phi} \tag{4}$$

$$R_{\parallel} = \frac{n_2 \cos \theta - n_1 \cos \phi}{n_2 \cos \theta + n_1 \cos \phi}. \tag{5}$$

For internal reflection, i. e., when the light approaches the interface from the denser medium, both $R_{\perp}$ and $R_{\parallel}$ become 100 percent at the critical angle θ_c, given by

$$\theta_c = \sin^{-1}\left(\frac{n_2}{n_1}\right) = \sin^{-1} n_{21} \tag{6}$$

where $n_{21} \equiv n_2/n_1$.

For angles of incidence larger than θ_c, ϕ becomes imaginary. In this case, the refracted angle ϕ may be obtained from the relation

$$\cos\phi = \left(1 - \sin^2\phi\right)^{\frac{1}{2}}$$

or

$$\cos\phi = i\ \frac{(\sin^2\theta - n_{21}^2)^{\frac{1}{2}}}{n_{21}} . \tag{7}$$

Substituting Equation 7 into Equations 4 and 5, the Fresnel reflection equations become

$$R_\perp = \frac{\cos\theta - i(\sin^2\theta - n_{21}^2)^{\frac{1}{2}}}{\cos\theta + i(\sin^2\theta - n_{21}^2)^{\frac{1}{2}}} \tag{8}$$

and

$$R_{||} = \frac{n_{21}^2\cos\theta - i(\sin^2\theta - n_{21}^2)^{\frac{1}{2}}}{n_{21}^2\cos\theta + i(\sin^2\theta - n_{21}^2)^{\frac{1}{2}}} . \tag{9}$$

Then, when n_{21} is real (i.e., when the media are transparent, or nonabsorbing), the reflection is total for angles of incidence between θ_c and 90 degrees.

If the rarer medium is absorbing, the reflectivity can be calculated by substituting in Equations 8 and 9 the complex refractive index for n_2, i.e.,

5

$$\tilde{N}_2 = n_2 + i\, k_2 \quad . \qquad\qquad (10)$$

The absorption coefficient, α, is related to the extinction coefficient, k, by

$$k = \frac{\alpha\lambda}{4\pi} \qquad\qquad (11)$$

where λ is the wavelength at which k is determined.

The Fresnel equations become complicated upon substitution of the complex refractive index and the use of a computer is necessary for solution of the equations.

The rarer absorbing medium strongly affects the reflectivity for internal reflection, particularly in the vicinity of the critical angle. The critical angle is no longer as sharp as it is with a non-absorbing medium; the reflectivity curves become less steep in this region, as shown in Figure 1. The absorption loss is quite large near the critical angle, is greater for parallel polarization than it is for perpendicular polarization, and decreases with increasing angle of incidence for both polarizations.

This behavior is the basis for attenuated total reflectance (ATR) spectroscopy, since the internal reflection, particularly in the vicinity of the critical angle, may be extremely sensitive to changes in the absorption coefficient.

In ATR, the reflection loss is the parameter measured. It is convenient to define an absorption parameter, a, as the reflection loss per reflection; i.e., for a single reflection,

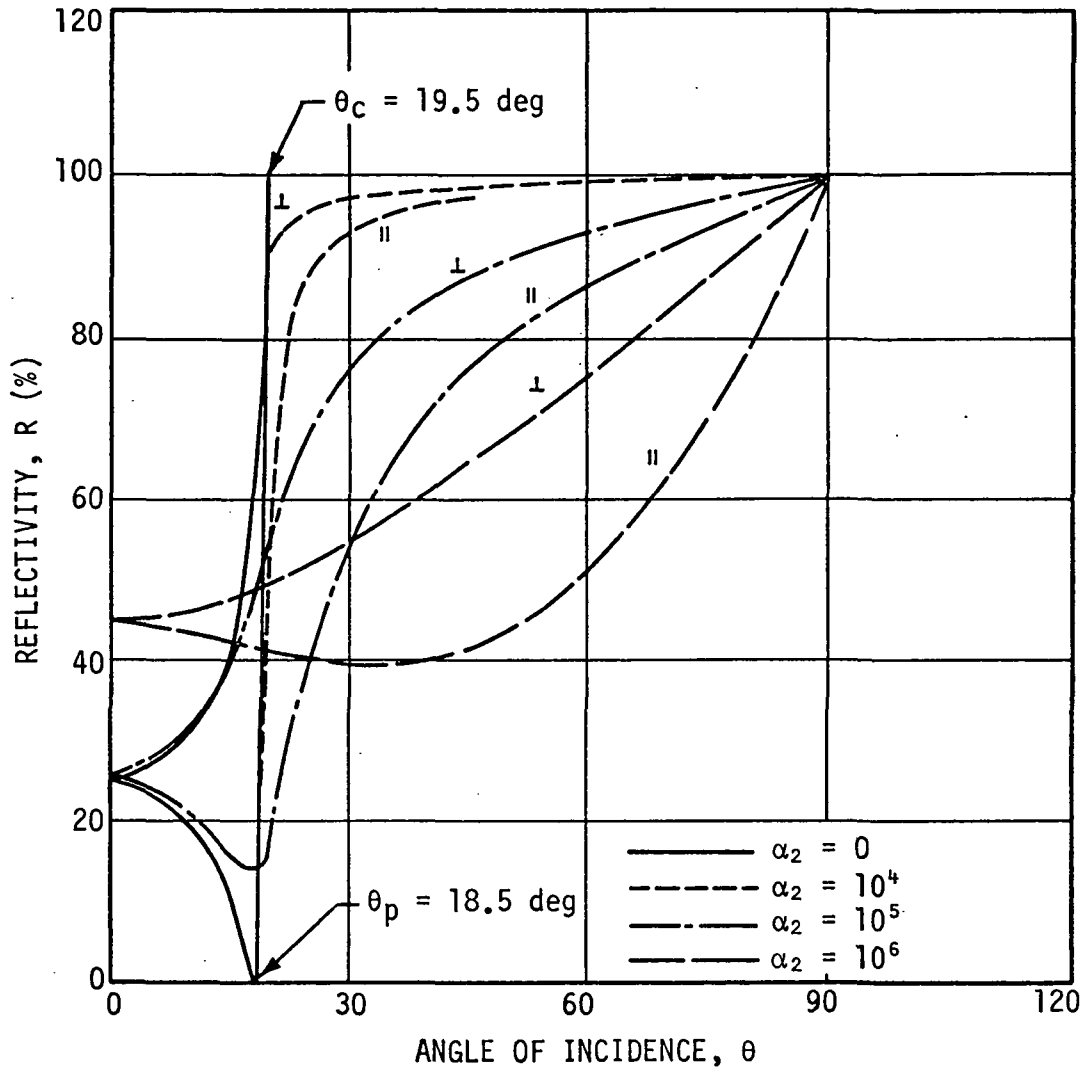$$R = 1 - a \quad . \qquad\qquad (12)$$

6

FIGURE 1. INTERNAL REFLECTIVITY OF AN INTERFACE VERSUS ANGLE OF INCIDENCE AT $\lambda = 0.4$ μ FOR $\eta_{21} = 0.333$ AND VARIOUS VALUES OF ABSORPTION COEFFICIENT α_2

It is useful to set up the equations for ATR in such a manner as to be directly comparable to transmission spectroscopy. For a material of actual thickness, d, and with an absorption coefficient, α, the transmittance, T, is given by

$$T = \exp(-\alpha d) . \qquad (13)$$

For $\alpha d \ll 1$,

$$T \approx 1 - \alpha d . \qquad (14)$$

Equations 14 and 12 are of the same form. It is convenient to define an "effective thickness", d_e, such that

$$R \equiv 1 - \alpha d_e \qquad (15)$$

where

α –   true absorption coefficient

d_e –   parameter, dependent on the optical properties of the media involved and the angle of incidence and polarization of the radiation incident on the media interface, which gives the correct R for the specified conditions.

Thus for N internal reflections

$$R^N = (1 - \alpha d_e)^N .$$

Equations 14 and 15 are useful for comparing the measured quantities R and T for known film thickness and effective thickness. However, if $\alpha d \gtrsim 1$, it is necessary to compare R and T obtained from

8

Equation 14. To relate the effective thickness to the actual film thickness, it is necessary to consider the establishment of standing waves at the reflecting interface.

It can be shown from Maxwell's equations that standing waves are established normal to a totally reflecting surface because of the superposition of the incoming and reflected waves (Ref. 1). For total internal reflection, there is a sinusoidal variation of the electric field amplitude with distance from the surface in the denser medium. By selecting the proper angle of incidence, it is possible to locate the antinode (the electric field maximum) at the surface and thus obtain the most efficient energy transfer across the interface. An evanescent wave exists in the rarer medium whose electric field amplitude decays exponentially with distance from the surface (see Figure 2). Consequently, one can define a depth of penetration, d_p as the distance required for the electric field, E, to fall to $1/e$ of its d_p value at the surface, E_0, i.e.,

$$E = E_0 \exp(-z/d_p) . \tag{16}$$

The depth of penetration is given by

$$d_p = \frac{\lambda_1}{2\pi} (\sin^2 \theta - n_{21}^2)^{-\frac{1}{2}} \tag{17}$$

where $\lambda_1 = \lambda/n_1$ is the wavelength in the denser medium and θ is the angle of incidence at the interface.

Assuming low absorption (i.e., $\alpha d < 0.1$), the effective thickness is calculated from the electric fields for zero absorption and is (Ref. 2)
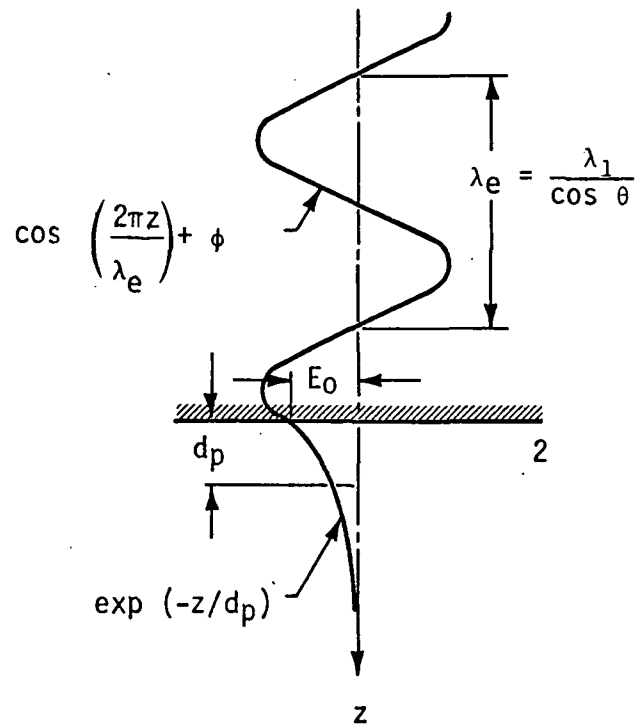
9

FIGURE 2. STANDING-WAVE AMPLITUDES ESTABLISHED NEAR
A TOTALLY REFLECTING INTERFACE (Ref. 1)

$$d_e = \frac{n_{21}}{\cos \theta} \int_0^d E^2 (z) \, dz \qquad (18)$$

where z is the distance in the rarer medium and d is the thickness of the medium, and E(z) is the electric field amplitude of the incident radiation within the sample. Substituting for E and solving, one obtains

$$d_e = \frac{n_{21}}{\cos \theta} \frac{E_o^2 \, d_p}{2} [1 - \exp(-2d/d_p)] . \qquad (19)$$

When $d \ll d_p$, d_e is given by

$$d_e = \frac{n_{21} \, E_o^2 \, d}{\cos \theta} \qquad (20)$$

while for $d \gg d_p$, d_e is given by

$$d_e = \frac{n_{21} \, E_o^2 \, d_p}{2 \cos \theta} . \qquad (21)$$

These equations indicate that four factors influence the strength of coupling of the evanescent wave with the absorbing medium. These four factors are the depth of penetration, d_p, the electric field strength at the interface, E_o, the sampling area and the refractive index matching.

The great advantage of ATR spectroscopy is that because of a reflectance of 1 for nonabsorbing media, many reflections can be utilized without reflection losses. Hence, small absorption losses for weakly absorbing films can be multiplied many times without a simultaneous increase in "noise" due to substrate reflection inefficiencies.

As mentioned before for N reflections, the measure reflectivity is

$$R^N = (1 - \alpha d_e)^N .$$

(22)

For $\alpha d_e < 0.1$

$$R^N \approx 1 - N \alpha d_e .$$

(23)

Then to maximize the absorption contrast, the product $N d_e$ should be maximized. Since d_e depends on the polarization of the incident radiation, it is convenient to consider the components perpendicular and parallel to the angle of incidence separately. Harrick (Ref. 3) has calculated the electric field amplitudes near a totally reflecting, non-absorbing interface. The equations for a maximum amplitude of unity are:

$$E_{yo} = \frac{2 \cos \theta}{(1 - n_{21}^2)^{\frac{1}{2}}}$$

(24)

$$E_{xo} = E_{yo} \frac{(\sin^2 \theta - n_{21}^2)^{\frac{1}{2}}}{\left[(1 + n_{21}^2) \sin^2 \theta - n_{21}^2\right]^{\frac{1}{2}}}$$

(25)

and

$$E_{zo} = E_{yo} \frac{\sin \theta}{\left[(1 + n_{21}^2) \sin^2 \theta - n_{21}^2\right]^{\frac{1}{2}}} .$$

(26)

The perpendicular and parallel components are given by

$$E_\perp = E_{yo} \tag{27}$$

$$E_{||} = (|E_{xo}|^2 + |E_{zo}|^2)^{\frac{1}{2}} . \tag{28}$$

Substituting Equations 27 and 28 for E_0 in Equation 19, one obtains

$$d_{e\perp} = \frac{4 n_{21} \cos \theta}{(1 - n_{21}^2)} \frac{d_p}{2} [1 - \exp(-2d/d_p)] \tag{29}$$

and

$$d_{e||} = d_{e\perp} \frac{(2 \sin^2 \theta - n_{21}^2)}{[(1 + n_{21}^2) \sin^2 \theta - n_{21}^2]} . \tag{30}$$

Note that since d_p is wavelength dependent (Equation 17), both $d_{e\perp}$ and $d_{e||}$ will increase with wavelength when d is not small relative to the wavelength of the incident radiation.

For most practical multiple reflection cell designs that retain the initial polarization, the number of reflections, N, is proportional to cot θ, so that

$$Nd_{e\perp} \propto d_{e\perp} \cot \theta \tag{31}$$

and

$$Nd_{e||} \propto d_{e||} \cot \theta . \tag{32}$$

13

To maximize the observed change in reflectance, one should maximize Equation 31 when using perpendicularly polarized radiation and Equation 32 when using parallel polarized radiation.

Equations 29 and 30 are general within the low absorption approximation. However, it must be pointed out that when medium 2 is very thin, the electric field amplitudes are determined by media 1 and 3 (Figure 3) and for this condition,

$$E_{\perp} = \frac{2 \cos \theta}{(1 - n_{31}^2)^{\frac{1}{2}}} \tag{33}$$

$$E_{||} = E_{\perp} \frac{[(1 + n_{31}^4) \sin^2 \theta - n_{31}^2]^{\frac{1}{2}}}{[(1 + n_{31}^2) \sin^2 \theta - n_{31}^2]^{\frac{1}{2}}} \tag{34}$$

so that

$$Nd_{e\perp} \propto \frac{4 n_{21} \cos \theta \cot \theta}{(1 - n_{31}^2)} \frac{d_p}{2} [1 - \exp(-2d/d_p)] \tag{35}$$

and

$$Nd_{e||} \propto Nd_{e\perp} \frac{[(1 + n_{31}^4) \sin^2 \theta - n_{31}^2]}{[(1 + n_{31}^2) \sin^2 \theta - n_{31}^2]} . \tag{36}$$

For a given sample material n_2 is fixed. Then to obtain maximum sensitivity, one must select the combination of θ, n_3, and n_1 which will optimize Equation 31 or Equation 35 when working with perpendicularly polarized light or Equation 32 or Equation 36 when working with parallel polarized light.
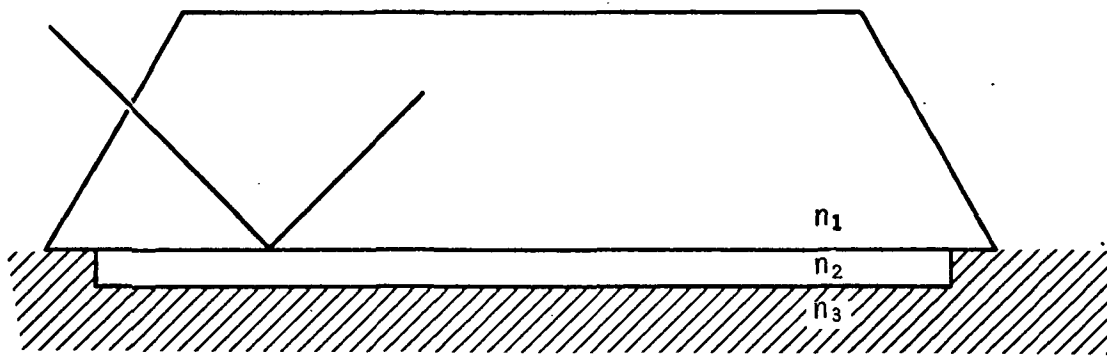
14

FIGURE 3. REFLECTION AT INTERFACE OF MEDIA

The internal reflection element (IRE) is a transparent (for the wavelength region under consideration) optical element used in internal reflection spectroscopy for establishing the conditions necessary to obtain internal reflection spectra of materials (Refs. 4 and 5). The ease of obtaining an internal reflection spectrum and the information obtained from the spectrum are determined by a number of characteristics of the IRE. A choice must be made in the working angle, number of reflections, aperture, number of passes, and the material from which it is made. These can be determined with some knowledge of the sample to be studied.

The aperture of the IRE is defined as the portion of the beveled area which can be utilized to conduct the light into the IRE at the desired angle of incidence θ. The apertures are given by

$$A = t \csc \theta \qquad \text{for } \theta \geq 45 \text{ deg}$$

$$A = 2t \sin \theta \qquad \text{for } \theta < 45 \text{ deg}.$$

Aperture is plotted against angle of incidence in Figure 4. It rises from zero at normal incidence to a maximum at 45 degrees, where it has a value of 1.414 times the IRE thickness t, and then decreases to a value equal to the thickness at grazing incidence.

The number of reflections is calculated from simple geometrical considerations. The beam of light advances a distance (skip distance) of $t \tan \theta$ for each reflection. If the plate length is ℓ, the total number of reflections for a single pass in the plate is given by

$$N = (\ell/t) \cot \theta .$$

A curve showing the dependence of N upon θ also appears in Figure 4. N is zero for grazing incidence, increases for decreasing θ, and
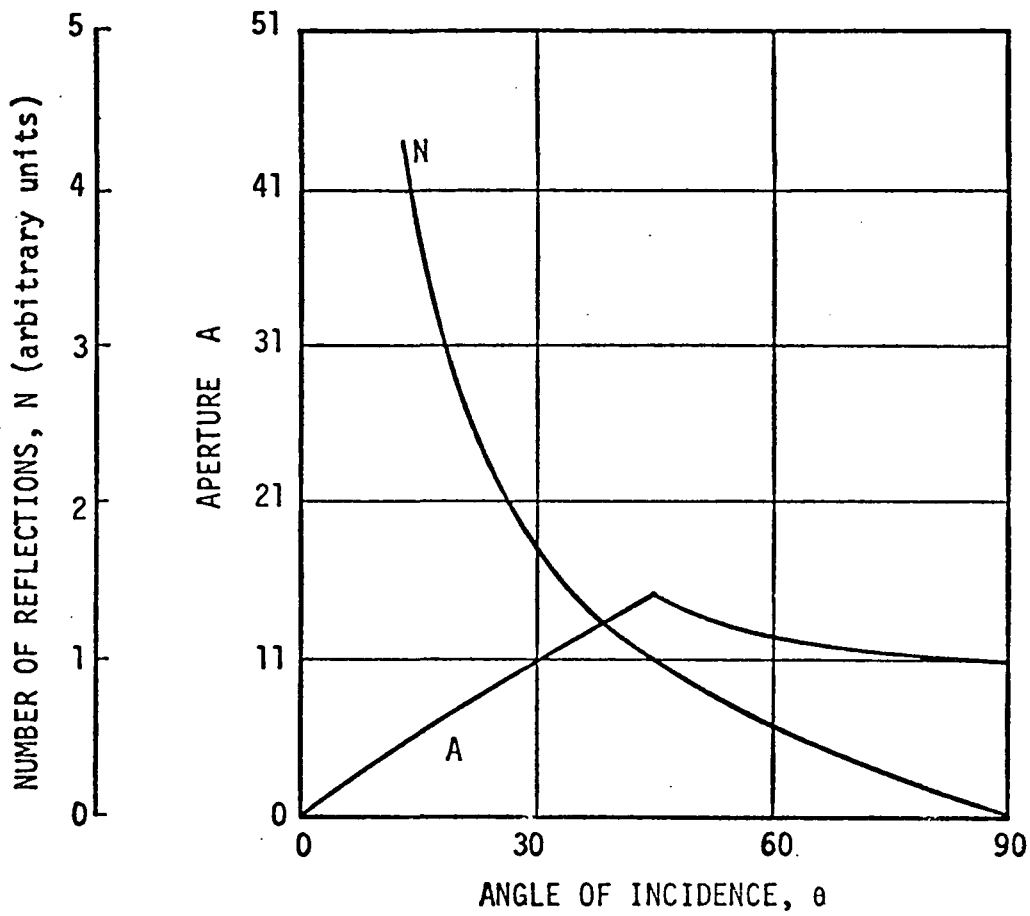
16

FIGURE 4. CALCULATED ANGULAR DEPENDENCE OF
APERTURE AND NUMBER OF REFLECTIONS
FOR SINGLE-PASS MULTIREFLECTION
ELEMENT

rises sharply for small angles. N also increases as the element is made longer and thinner. Because of the practical considerations, there are limitations on both ℓ and t. Moreover, θ must be greater than the critical angle. Another consideration is that a decrease of either θ or t reduces the aperture and this limits the usable light beam width, hence power, that can be employed. For these reasons, N cannot be made indefinitely large. For single pass elements, the approximate upper limit of N is 10^3.

EXPERIMENTAL

KRS-5 was selected as the internal reflection element (IRE) because its infrared transmission range falls well within the wavelength region of present investigations. The dimensions of the KRS-5 plate was chosen as 5.25 by 1.0 by 0.2 centimeters thick. The faces were cut to get a 45-degree angle of incidence. This geometry of the IRE gives a minimum of 25 internal reflections and was adequate for the present study. The contaminants were deposited on the IREs for measuring their infrared spectra.

The infrared spectra of the contaminants were recorded using a Beckmann Microspec Infrared Spectrophotometer. Although this is a double-beam instrument, only a single-beam mode of operation was used for the present study. Monochromatic radiation from the Microspec was focused onto the KRS-5 crystal face. The emerging radiation from the other face of the crystal was collected by two fast mirrors and focused onto the detector. The optical diagram of the measuring system is shown in Figure 5. The spectra of the contaminants were recorded by scanning the Microspec at a typical speed of 1 inch per minute. All measurements were done with the contaminants exposed to atmosphere.

The contamination chamber used to deposit the contaminants onto the IREs is shown in Figure 6. It consists of a glass cross with a quartz window at one end. The other end is closed with an aluminum plate using an O-ring seal and flange. The top cover and the cold finger is made of brass. The bottom end of the cross goes to the pumping system. Only a cryopump and ion pump were used to avoid any contamination that might result from the use of an oil diffusion pump.
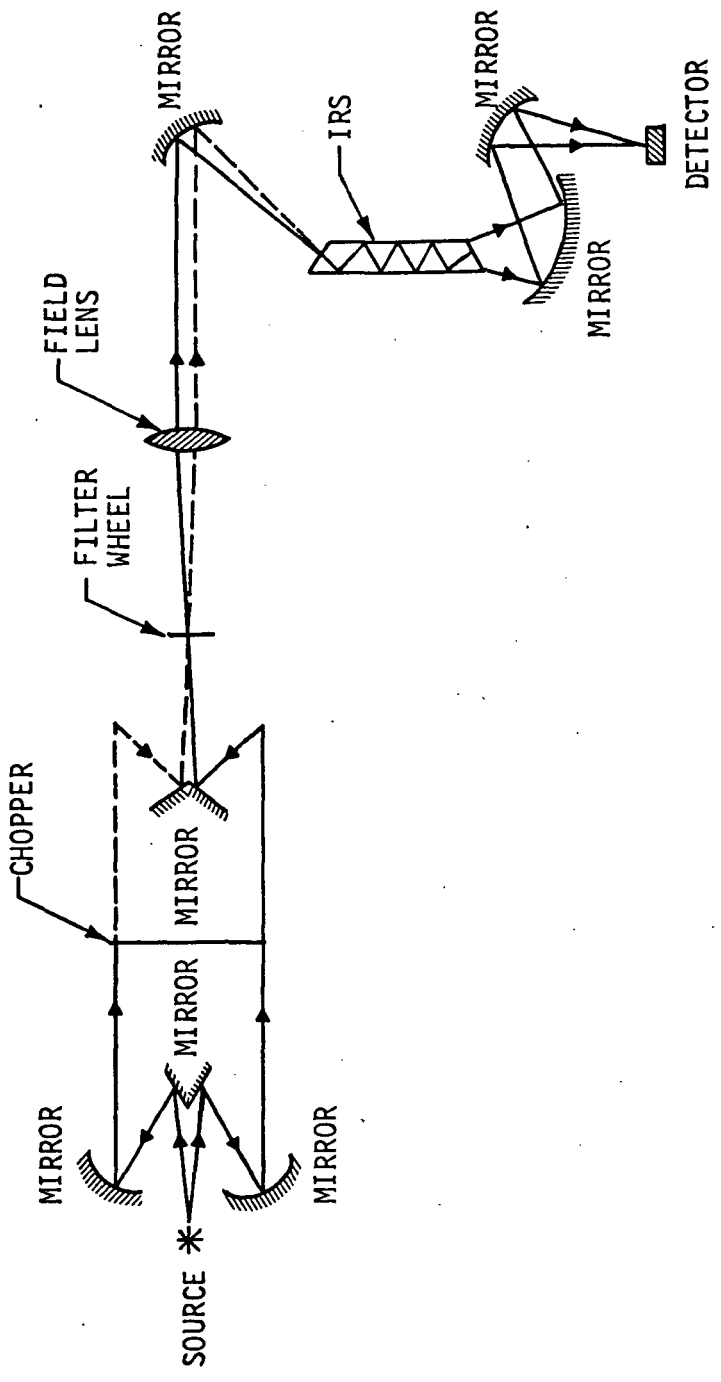
FIGURE 5. OPTICAL DIAGRAM OF MEASURING SYSTEM
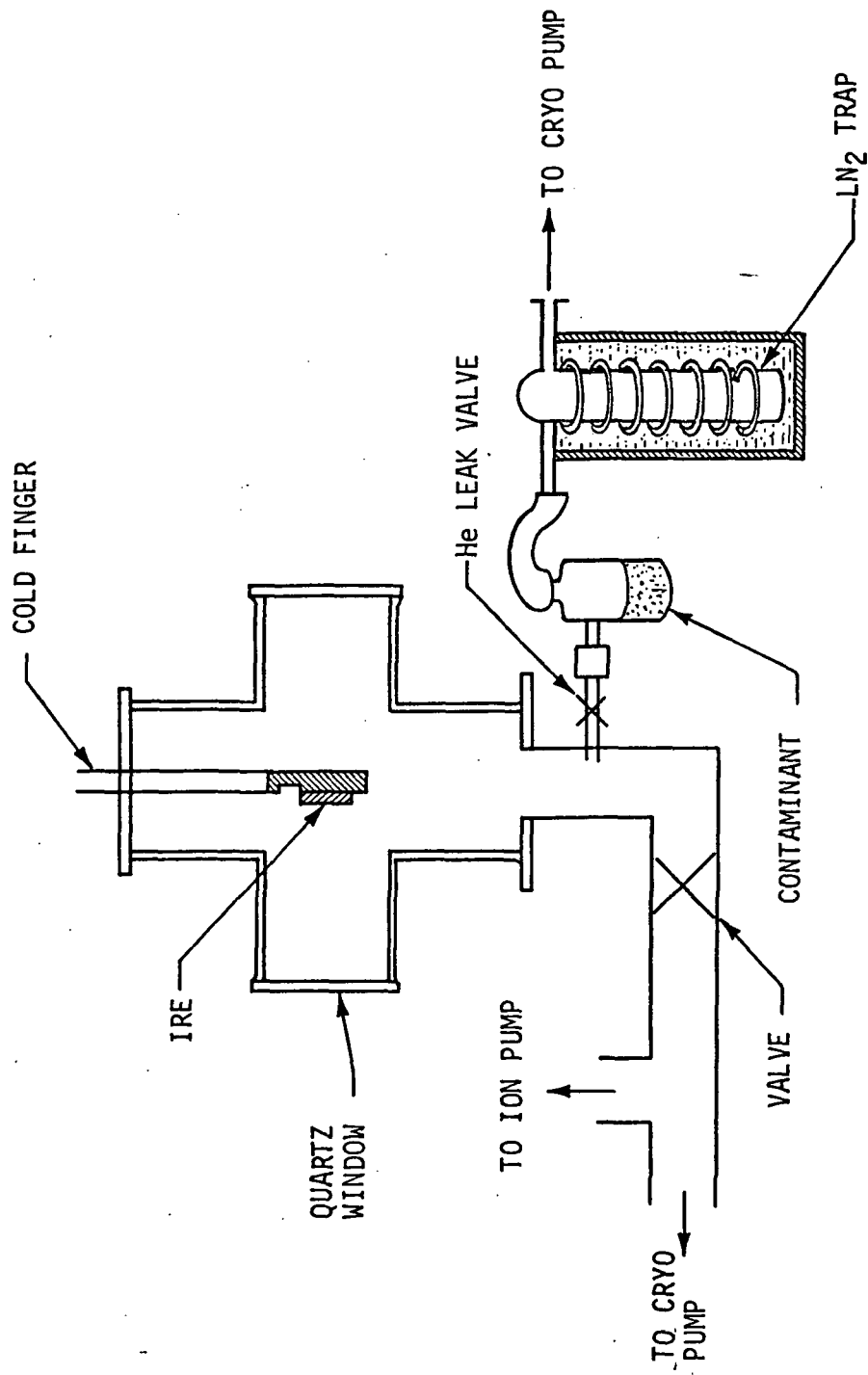
FIGURE 6. CONTAMINATION CHAMBER

The system was pumped down to 10^{-4} torr before the contamination of the IREs. The IRE mounted on the cold finger was cooled using liquid nitrogen. The vessel containing the contaminant was also pumped for a few seconds through the liquid nitrogen trap to remove the atmosphere in that assembly. The contaminant was then introduced into the chamber by opening the helium leak valve.

The contaminants were irradiated with ultraviolet radiation through the quartz window of the contamination chamber. A xenon-mercury lamp was used for this purpose. Infrared spectra of the contaminants were recorded both before and after irradiation.

RESULTS AND DISCUSSION

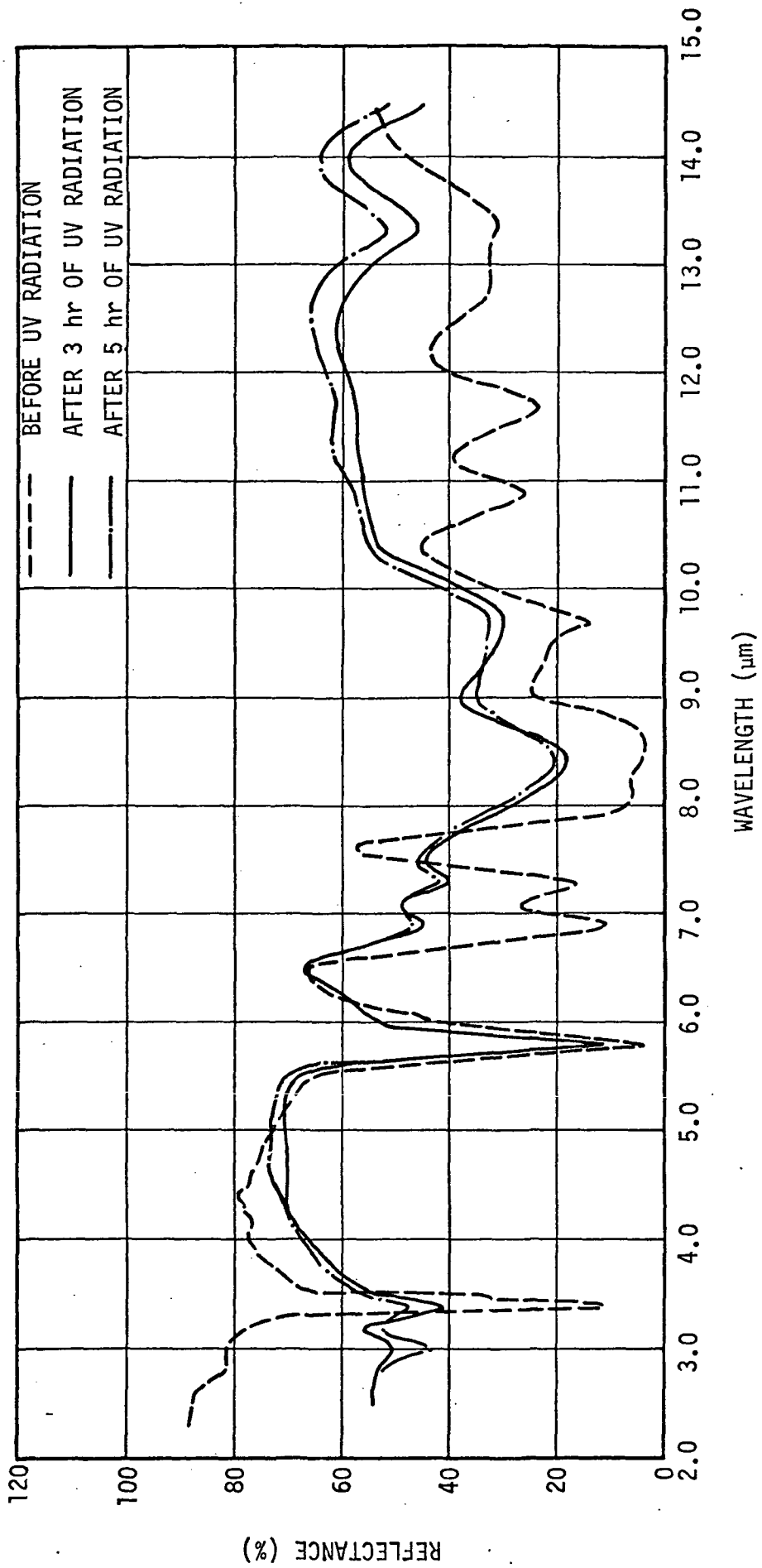The results of the present study are presented in Figures 7 through 20, where the amount of optical radiation reflected through the IRE is plotted as a function of the wavelength for each material, both before and after ultraviolet irradiation. Each material studied is discussed separately. First the monocomponent systems are discussed, then the binary mixtures.

MONOCOMPONENT SYSTEMS

Diethyl Adipate

This material is the ester of adipic acid and its chemical structure is

$$
\begin{array}{c}
\quad\;\; H \quad H \quad\; O \qquad H \quad H \\
\quad\;\; | \quad\;\; | \quad\;\; \| \qquad | \quad\;\; | \\
H - C - C - C - O - C - C - H \\
\quad\;\; | \qquad | \qquad\qquad | \quad\;\; | \\
\quad\;\; | \qquad H \qquad\qquad H \quad H \\
\quad\;\; | \qquad H \qquad\qquad H \quad H \\
\quad\;\; | \qquad | \qquad\qquad | \quad\;\; | \\
H - C - C - C - O - C - C - H \\
\quad\;\; | \qquad | \quad\; \backslash\quad\;\; | \quad\;\; | \\
\quad\;\; H \quad H \quad\;\; O \qquad H \quad H
\end{array}
$$

The infrared spectrum of this ester is shown in Figure 7. Diethyl adipate has its characteristic CH_2 and CH_3 absorption at 3.4 micrometers. The absorption band at 5.8 micrometers is due to carbonyl $C = 0$. The CH_2 scissor deformation and CH_3 asymmetric deformation band for the diethyl adipate molecule appears at 5.9 micrometers. The band at 7.30 micrometers is due to the $C-CH_3$ vibration. The C-O band present in this molecule should have its stretching vibration adsorption around 8.0 micrometers. Also the CH_2 present in this structure should have absorption due to its wag around the same wavelength. The double hump at 8.05 micrometers and 8.50 micrometers observed in the present case is probably because of these two kinds of vibrations. The absorption band at 11.7 micrometers is probably due to C-O-C vibration.

FIGURE 7. SPECTRA OF DIETHYL ADIPATE

The chart legend shows:
- BEFORE UV RADIATION
- AFTER 3 hr OF UV RADIATION
- AFTER 5 hr OF UV RADIATION

Axes:
- Vertical: REFLECTANCE (%), scale from 0 to 120
- Horizontal: WAVELENGTH (μm), scale from 2.0 to 15.0

24

Ultraviolet irradiation has a pronounced effect on this material. It can be seen from Figure 7 that all the bands except that at 5.8 micrometers are drastically reduced to ultraviolet and a new band appears at 3.0 micrometers and around 14.5 micrometers. This suggests that there is scission of bands joined to the C=0 group and radical fragments are formed which could undergo combination and disproportion reactions.

The mass resulting from ultraviolet irradiation was difficult to remove from the IRE surface.

Trioctyl Phosphine

The chemical structure of this organic compound is

$$\left[CH_3 \ (CH_2)_7 \right]_3 \ P \ .$$
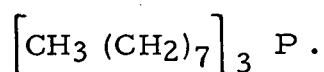
The infrared spectrum of this material is shown in Figure 8. The aliphatic CH_3 and CH_2 present in this compound show their characteristic absorption at 3.4 micrometers. This is a doublet with about 0.1-micrometer separation. The CH_2 deformation of the CH_2 group which is next to the phosphorus is seen to absorb at 6.85 micrometers. The band at 14.0 micrometers is probably due to CH_2 rocking vibration. Trioctylphosphine is a very strong reactive material and reacts with moisture in air. The other bands are probably due to this reason. The bands at 6.05 micrometers and at 10.05 micrometers observed in the present case have been identified as due to the P-OH group.

Ultraviolet irradiation has a drastic effect on this material. A 15-minute exposure makes the surface black and opaque. This mass absorbs very strongly in the 2.5- to 5.0-micrometer range, and thus the C-H stretching band at 3.4 micrometers could not be observed. A new broadband around 7.3 micrometers also appears.
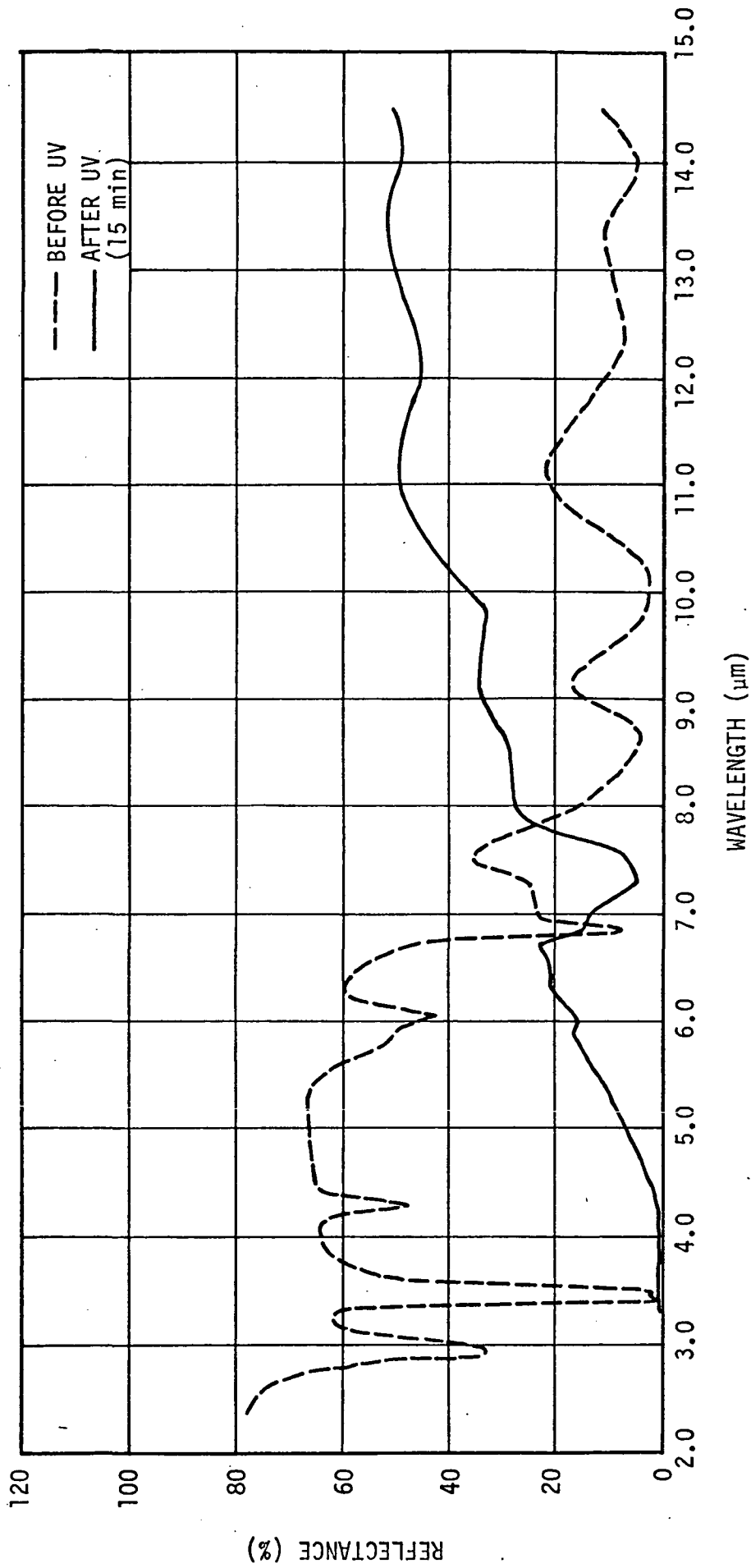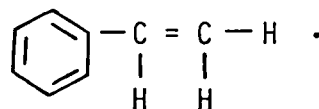
FIGURE 8. SPECTRA OF TRIOCTYLPHOSPHINE

26

The black mass resulting from ultraviolet irradiation could not be removed from the IRE surface. This indicates permanent bonding of this material with the IRE surface, probably because of crosslinking and polymerization.

Styrene

The chemical structure of mono styrene is

$$
\text{C}_6\text{H}_5 - \overset{\displaystyle |}{\underset{\displaystyle H}{C}} = \overset{\displaystyle |}{\underset{\displaystyle H}{C}} - H \; \cdot
$$

The infrared spectrum of this monomer is shown in Figure 9. This material evaporates very rapidly when exposed to atmosphere. Hence a good spectrum could not be obtained. Nevertheless, absorption due to the H stretching vibration of monosubstituted benzene can be seen at 3.32 micrometers. The aliphatic CH_2 band appears at 3.43 micrometers. The doublet character of this absorption band is not revealed in this spectrum. The C=C group present in the structure absorbs at 5.95 micrometers. The CH_2 scissors deformation probably appears at 6.9 micrometers. The in-plane and out-of-plane H bending bands appear at 7.95 micrometers and between 11.0 and 13.3 micrometers.

This material had to be ultraviolet-irradiated in air because styrene will evaporate from the IRE surface due to vacuum. Ultraviolet irradiation is found to increase the bulk absorption in the low wavelength region. The bands at 5.95 and 7.95 micrometers were found to increase. The bands at 3.32 and 3.43 micrometers got masked by the broad bulk absorption and lost their structure. The polymerization of styrene due to ultraviolet could not be seen properly because of the problem of evaporation of the material in air.
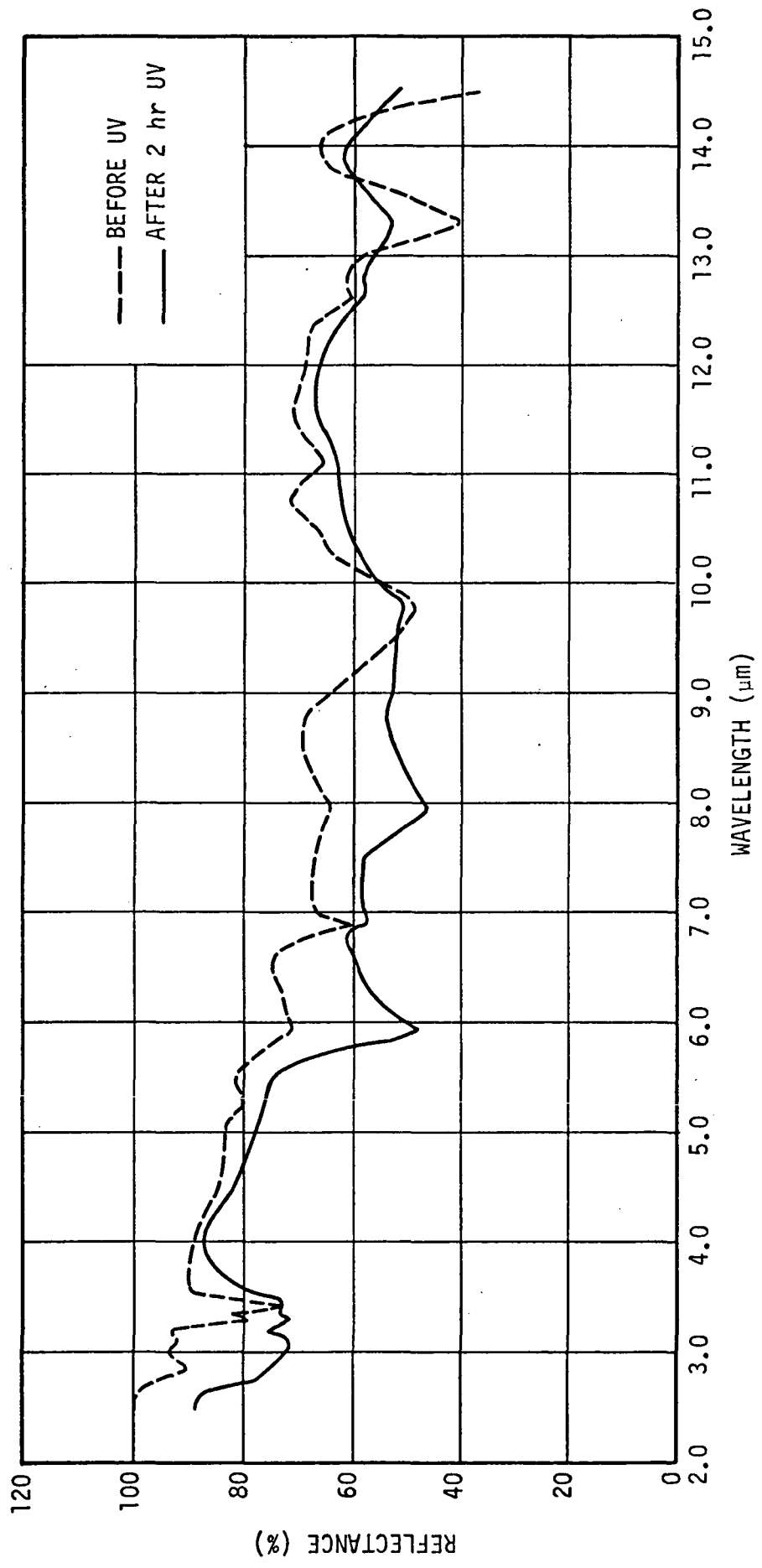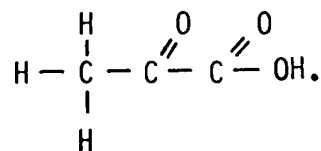
FIGURE 9. SPECTRA OF STYRENE

RTV-140

This is a sealent material made by Dow-Corning. It was deposited onto the IRE by desolving it in acetone. The infrared spectrum is shown in Figure 10. The strong absorption band at 3.38 micrometers is due to C-H stretching vibration of aliphatic CH_3 group. The doublet structure of this band could not be resolved. The strong absorption band at 7.98 micrometers is due to $Si-CH_3$. This vibration is further confirmed by the band at 11.6 micrometers which is due to Si-C stretching. The band at 11.6 micrometers also suggests that there are two and/or three CH_3 groups attached to the Si atom. The band at 12.65 micrometers is due to CH_3 rocking and Si-C stretching vibrations. Hence it can be said that the weak band at 7.1 micrometers is due to asymmetric CH_3 deformation. The strong double band extending from 9.0 to 10.0 micrometers is characteristic of Si-O-Si asymmetric stretching vibration. The infinite Si-O-Si chain has absorption maxima around 9.22 micrometers and 9.8 micrometers which matches up with the present measurement. All these assignments suggest that RTV-140 is a long chained methyl siloxane.

A 2-hour exposure of this material to ultraviolet radiation did not show appreciable change in the spectra.

Pyruvic Acid

This material is a human outgassing product. The chemical structure is

$$H - \overset{\overset{\displaystyle H}{|}}{\underset{\underset{\displaystyle H}{|}}{C}} - \overset{\overset{\displaystyle O}{\diagup\!\!\diagup}}{C} - \overset{\overset{\displaystyle O}{\diagup\!\!\diagup}}{C} - OH .$$
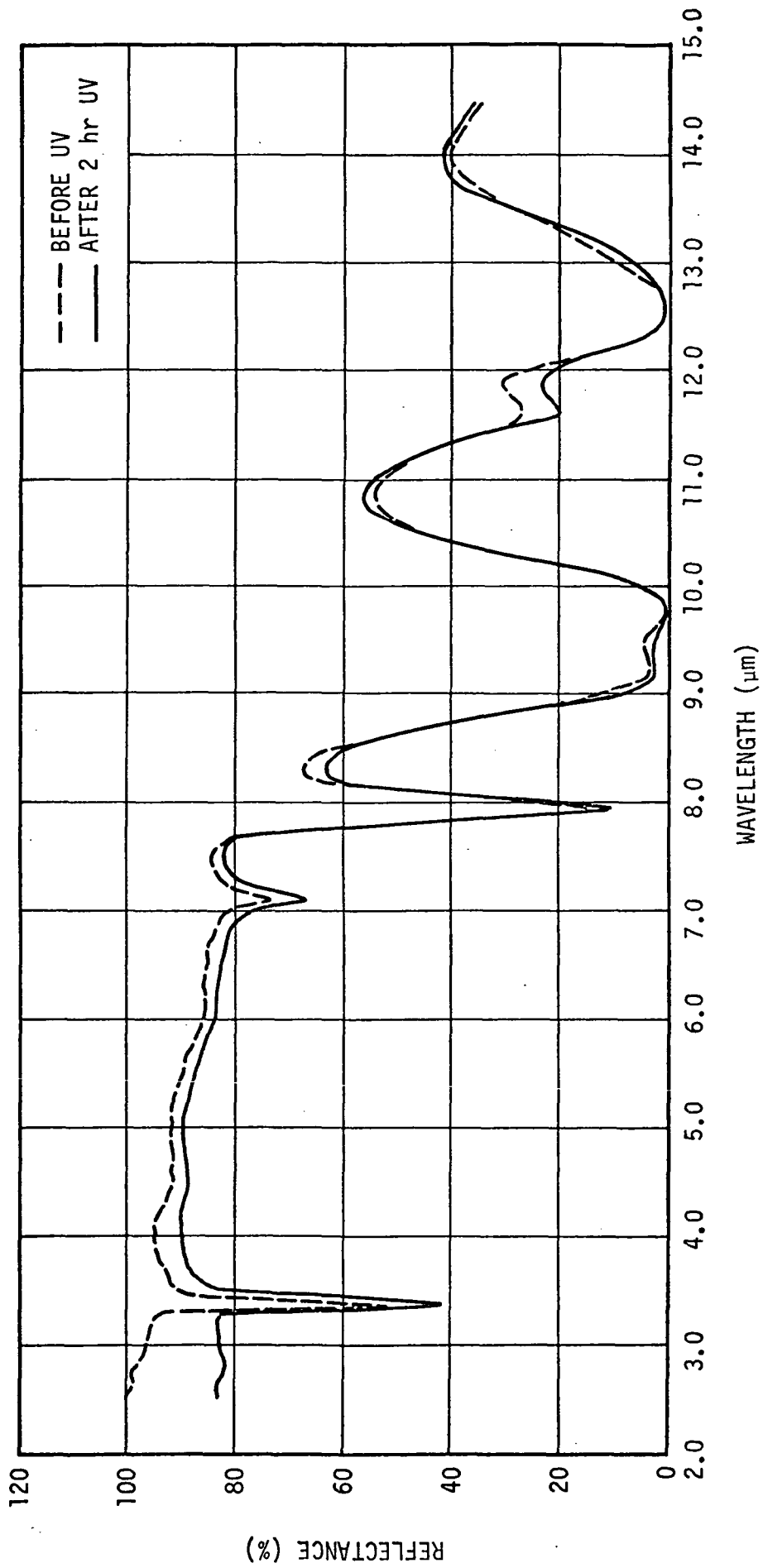
FIGURE 10. SPECTRA OF RTV-140

30

The infrared spectrum is shown in Figure 11. The double band centered around 3.0 micrometers is characteristic of pyruvic acid. This is a combination of very broad absorption due to the OH radical and the CH_3 present in the molecule. The strong absorption band at 5.72 micrometers is due to C=O of the acid. The weak and broad band around 7.0 micrometers is probably due to the asymmetric deformation of CH_3 which is close to a C=O group. The C-O stretch vibration has its band at 8.3 micrometers.

Exposure to ultraviolet radiation for 2 hours broadens and takes the structure out of the band around 3.0 micrometers. All the other bands are drastically reduced, and in turn, three new bands appear at 5.85, 6.25, and 6.7 micrometers. The band at 5.85 micrometers suggests a stretching vibration due to aldehydic C=O and the bands at 6.25 and 6.7 micrometers suggests the presence of a phenyl radical. Such a change of pyruvic acid due to ultraviolet irradiation is probably because of intramolecular fission of the C-C band.

The material that resulted after ultraviolet irradiation was very difficult to remove from the IRE surface.

Chlorotrimethylsilane

The chemical structure of this compound is

$$
\begin{array}{c}
CH_3 \\
| \\
H_3C - Si - Cl \,. \\
| \\
CH_3
\end{array}
$$
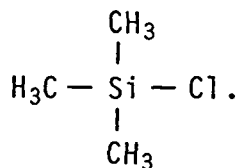
The infrared spectrum of this contaminant material is shown in Figure 12. The absorption band at 3.36 micrometers is the aliphatic C-H stretching vibration of the CH_3 group present in the molecule. The band at 7.98 micrometers is because of the presence of $Si-CH_3$.
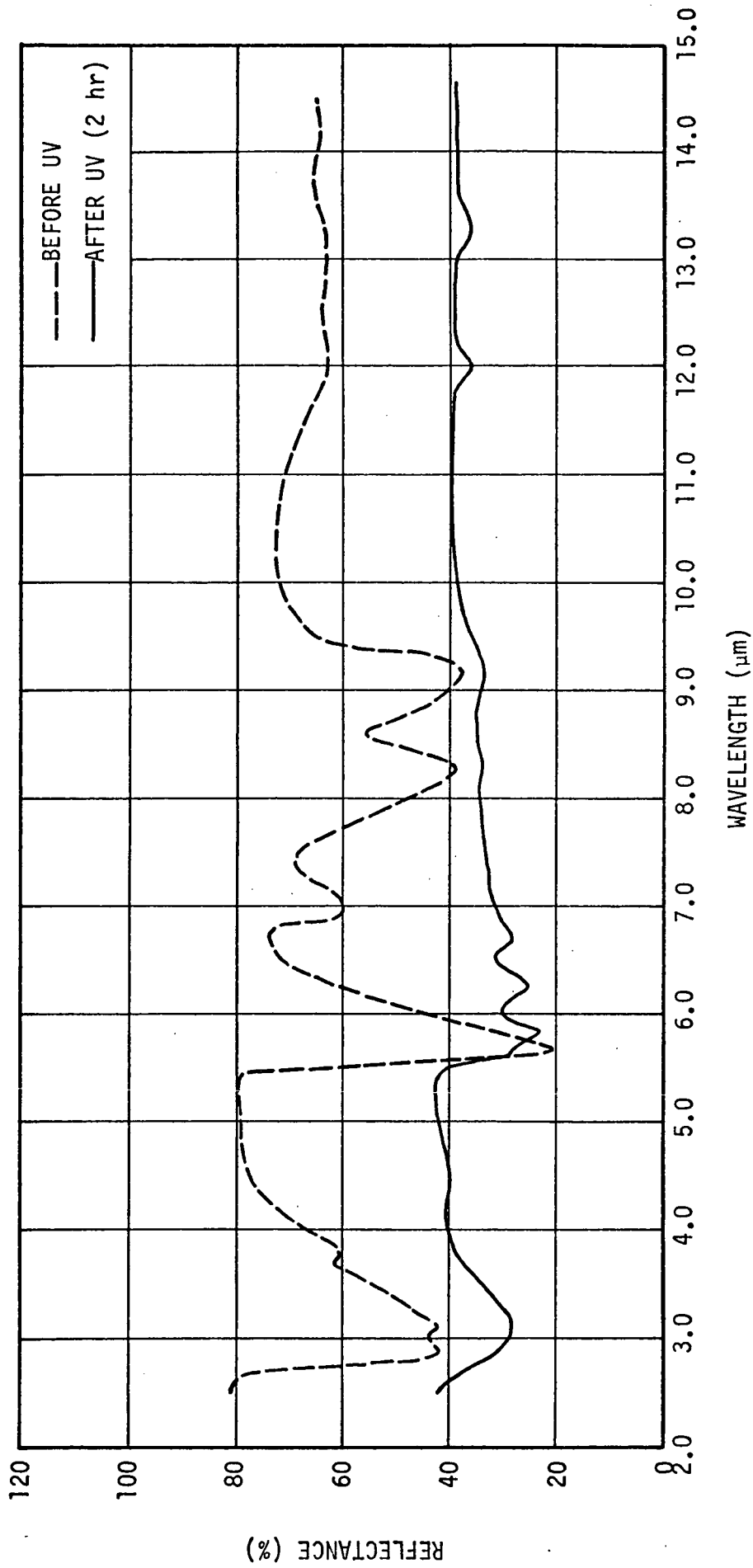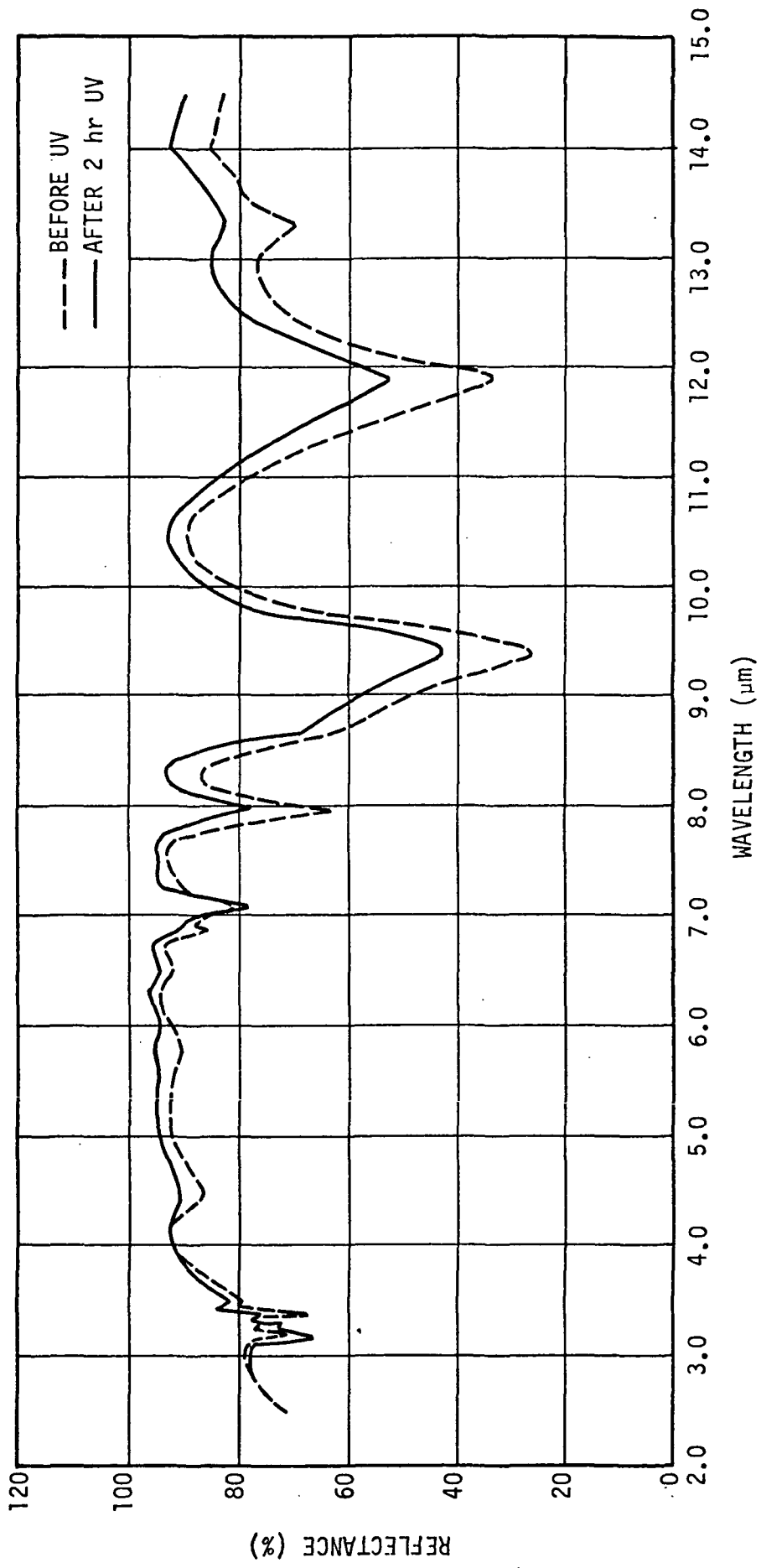
FIGURE 11. SPECTRA OF PYRUVIC ACID

FIGURE 12. SPECTRA OF CHLOROTRIMETHYLSILANE

The presence of the CH3 group is again evident due to the weak band at 7.1 micrometers. The CH3 rocking vibration and Si-C stretching vibration gives rise to the broad absorption band at 11.9 micrometers.

This material is very reactive when exposed to the atmosphere. The band at 9.4 micrometers observed in the present case is characteristic of Si-O-aliphatic and Si-O-Si. It is possible that this material, when exposed to atmosphere, reacts with the oxygen and moisture and forms a long chain of either Si-O-CH3 or Si-O-Si.

Under this condition, the study of the ultraviolet irradiation effects does not convey much meaning. The effect of ultraviolet on this material should be studied in situ, without exposing the material to atmosphere.

The material turns grey due to 2 hours of ultraviolet exposure and this grey mass is very difficult to remove from the IRE surface.

Dimethyl Phthalate

This compound is the ester of O-phthalic acid and its structural formula is

$$
\underset{\text{O}}{\underset{\|}{\underset{\|}{\text{O}}}}
$$
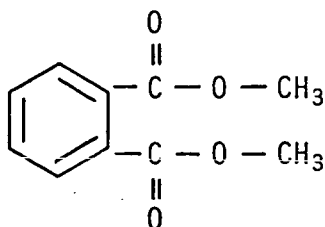
The infrared spectrum of this material is shown in Figure 13. This material is characterized by its unique absorption band at 5.8 micrometers. This band is due to the C=O stretching vibration. The doublet around 3.4 micrometers is due to the C-H stretching of the CH3 group present in the structure. This group which is next to the C=O group shows it asymmetric deformation absorption at 7.03 micrometers. The aromatic ring shows its presence through the absorption bands at 6.3,
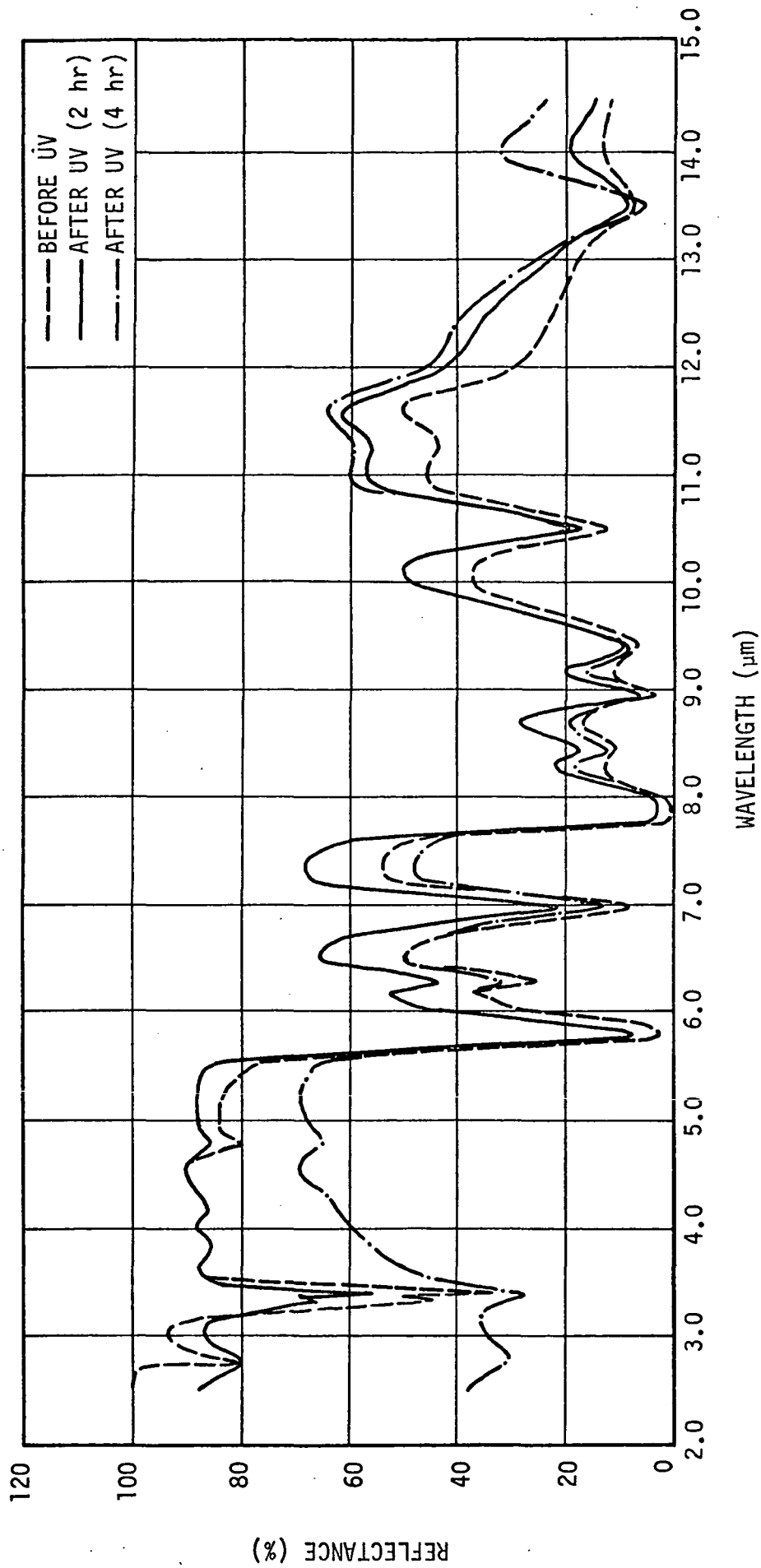
34

FIGURE 13. SPECTRA OF DIMETHYL PHTHALATE

35

8.45, and 9.4 micrometers. The four adjacent hydrogen atoms of the
other distribution absorbs at 13.5 micrometers. The band at 7.8
micrometers is due to C-O stretching vibration and C-$\overset{||}{C}$-O asymmetric
vibration. The C-O stretching vibration absorption is again shown at
8.95 micrometers.

Ultraviolet irradiation has drastic effect on this ester, as can
be seen from Figure 13. The CH_3 band on 3.4 micrometers decreases
significantly. After 4 hours of irradiation, the bulk absorption at shorter
wavelengths is high and the 3.4-micrometer band almost disappears.
This also gives higher transmission in the longer wavelength regions
and lower intensities for the absorption bands in this region. Excita-
tion of this ester molecule by ultraviolet probably results in band cleav-
age to form free radicals and intramolecular fission of the C-C band
and subsequent polymerization.

Polymerization is suspected in the present case since the greyish-
white mass resulting from ultraviolet irradiation could not be removed
from the IRE surface by organic solvents.

Urea

The structural formula of this compound is

$$H_2N - \overset{\overset{O}{||}}{C} - NH_2 \ .$$
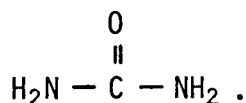
The infrared spectrum is shown in Figure 14. The NH_2 group gives its
absorption band at 3.0 micrometers . This is a strong band and charac-
teristic of the particular group. The band around 6.2 micrometers is due
to two kinds of absorption; one, with its peak around 6.0 micrometers, is
due to C=O stretching vibration, and the other, with peak at 6.3 micro-
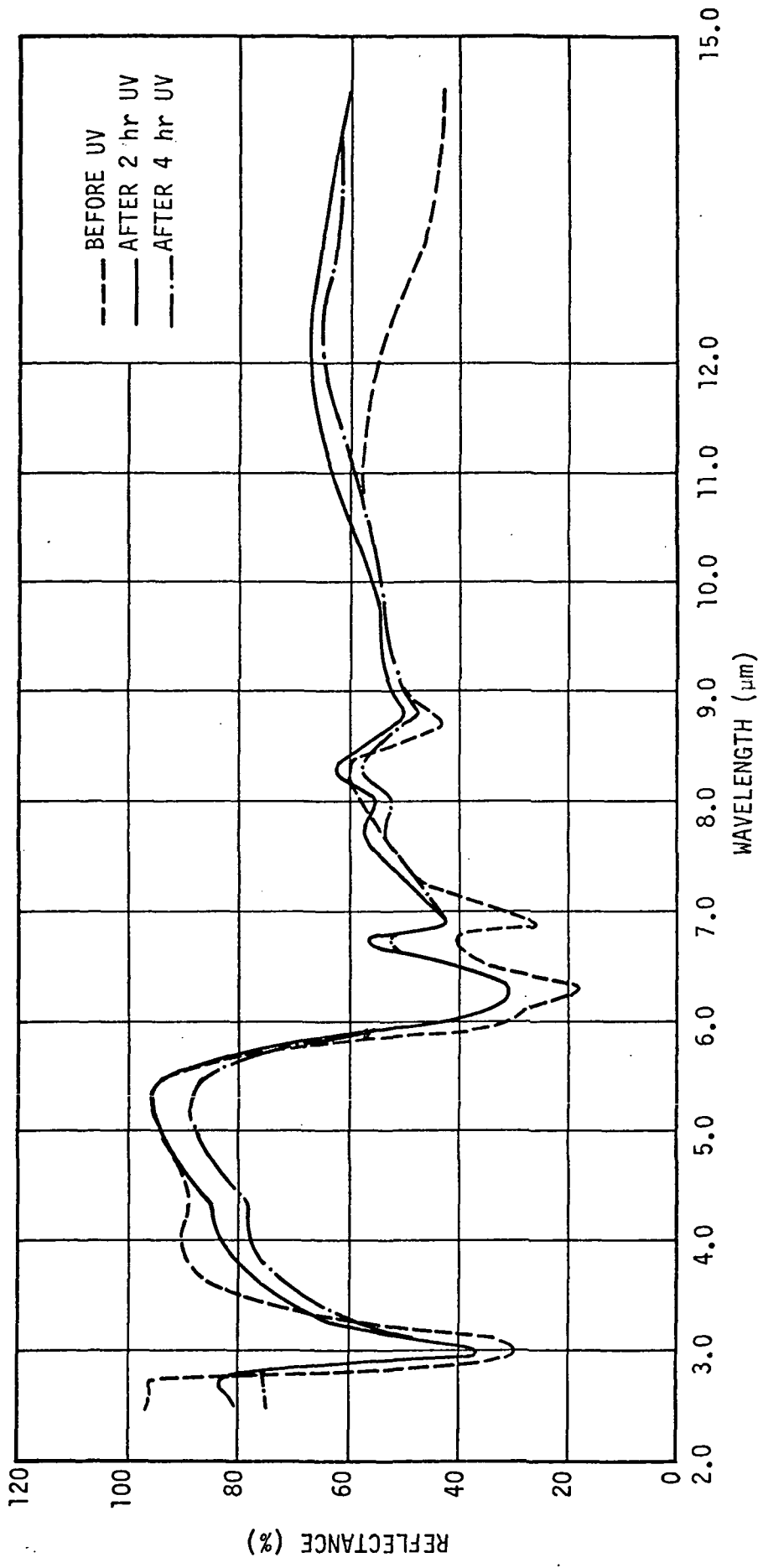meters, is because of NH_2 scissors deformation. The absorption due to
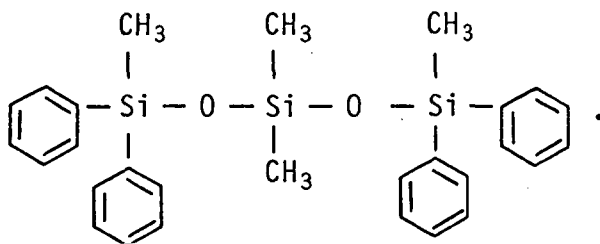
36

FIGURE 14. SPECTRA OF UREA

37

NH_2 rocking vibration probably appears at 8.7 micrometers. The band at 6.9 micrometers is believed to be due to C-N stretching vibration absorption.

Ultraviolet irradiation of this compound removed the shoulder around 6.0 micrometers and gives rise to a new band at 8.0 micrometers. Free radical formation by the C-N band cleavage probably occurs in this case. The radical fragments might undergo fission and polymerization. The appearance of the new band at 8.0 micrometers points in this direction.

This material evaporates rapidly when exposed to air, but the material resulting out of ultraviolet irradiation leaves a stain which does not evaporate, but can be removed by scrubbing with acetone-soaked cotton.

Tetramethyltetraphenyltrisiloxane (DC-704)

This is a diffusion pump oil and the structural formula is

$$\begin{array}{ccccccc} & CH_3 & & CH_3 & & CH_3 & \\ & | & & | & & | & \\ \bigcirc - & Si & - O - & Si & - O & - Si & - \bigcirc \\ & | & & | & & | & \\ & \bigcirc & & CH_3 & & \bigcirc & \end{array}$$

The infrared spectrum is shown in Figure 15. The double peak around 3.3 micrometers is due to the C-H stretching vibration of the aromatic ring and the aliphatic CH_3 group. The CH_3 deformation absorbs at 7.03 micrometers. The absorption due to Si-CH_3 shows its band at 7.98 micrometers. Another absorption of this group due to Si-C stretching is observed at 12.7 micrometers. The characteristic absorption due to the Si-O-Si asymmetric stretching vibration shows its peak at 9.6 micrometers. This band is broadened by the overlapping band due to
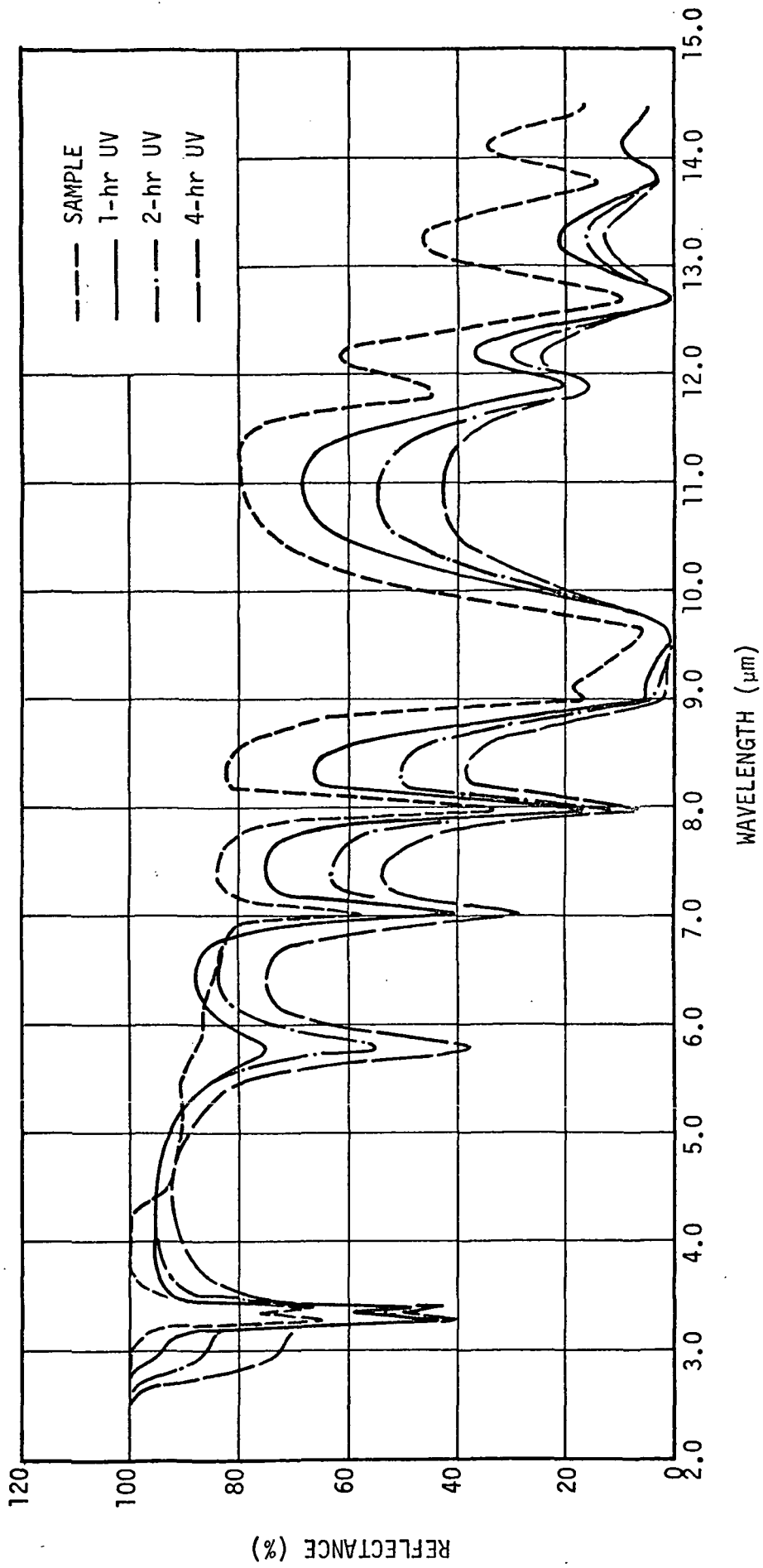
FIGURE 15. SPECTRA OF TRIMETHYLPENTAPHYENYLTRISILOXANE (DC-704)

39

the Si-O-CH$_3$ stretching absorption. Two CH$_3$ groups on a Si shows their characteristic absorption at 11.9 micrometers. Finally, the absorption band at 13.8 micrometers is due to the five adjacent hydrogen atoms of the monosubstituted benzene.

Figure 15 also shows the changes in different absorption bands due to 1, 2, and 4 hours of ultraviolet irradiation. As can be seen, two new bands start appearing: one around 3.0 micrometers and the other at 5.8 micrometers. All other bands lose their intensity. Various OH groups have their stretching vibration absorption in the region of 2.7 to 3.22 micrometers. Another group which absorbs near 3.03 micrometers is C=C-H. The strong new band at 5.8 micrometers is in general a characteristic absorption of the C=O group. It is likely that the Si-O-Si chain is cleaved and the broken fragments are undergoing disproportion reaction and polymerization to form a new compound. The resulting material could not be totally removed from the IRE surface by scrubbing with organic solvents.

Clean Room Samples

This sample was supplied by the technical COR. The material was obtained as a thin deposit on a microscope cover slide. For measurement of the infrared spectrum, the material was transferred to the IRE surface by pressing the microscope cover slide on it. The spectral run is shown in Figure 16. The absorption band at 3.4 micrometers is due to the C-H stretching of the CH$_3$ group. This group shows another absorption at 8.5 micrometers. The peak at 5.8 micrometers is characteristic of C=O.

The band at 8.1 micrometers could be due to C-O and/or Si-CH$_3$ stretching vibration. The absorption due to the C-O-C group is observed at 11.0 micrometers. The absorption band at 9.7 micrometers could be due to both C-O-C and Si-O-Si. Similarly, the band at 12 micrometers could be due to both C-O-C and Si-CH$_3$.
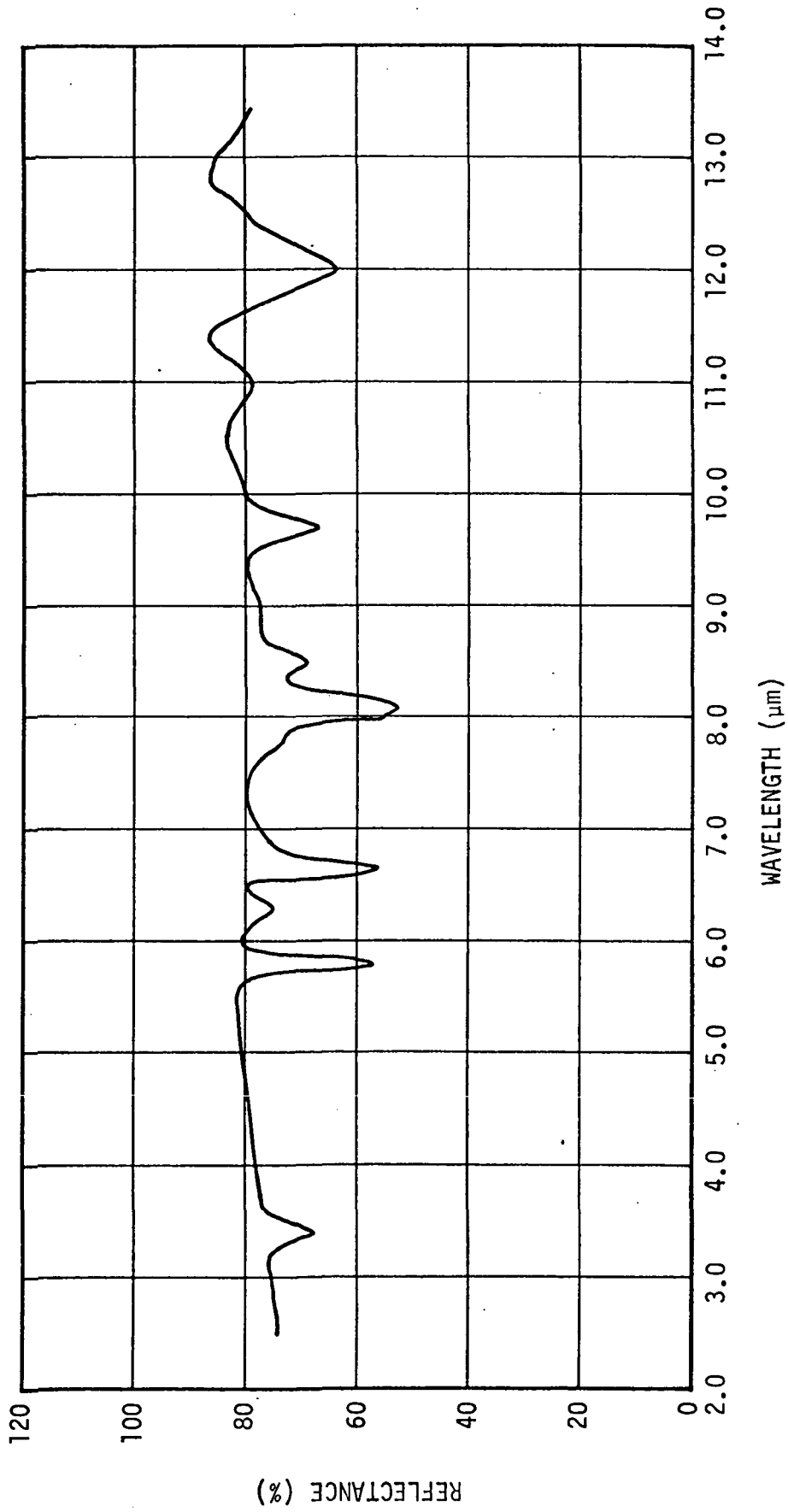
40

FIGURE 16. SPECTRA OF CLEAN ROOM SAMPLE

41

From all these observations, it appears that the clean room sample probably contains a mixture of a methyl siloxane and an ester of the phthalate type.

Water and alcohol, which are human outgassing products, could not be studied because they would not stay on the IRE surface when exposed to atmosphere at ambient temperatures. In situ measurements are very necessary to study the ultraviolet irradiation effects on these. Both these contaminants are expected to give rise to molecular fragmentation and free radical formation due to ultraviolet excitation.

The other two materials that could not be studied are hydrazine and monomethyl hydrazine. Both these materials are important from the contamination point of view because they are used as fuel in RCS engines. The reason for not being able to study these are; they react with the IRE material. Hence to study these materials, IREs made out of material other than KRS-5 should be used. IREs made out of germanium can be adequately used. The other reason is that they fume when exposed to atmosphere. Hence, in situ measurements will be most appropriate.

BINARY MIXTURE

Pyruvic Acid and Water

This mixture could not retain water molecules, under ambient conditions, as is evident from the infrared spectrum (Figure 17). This spectrum is the same as that for pyruvic acid. No water absorption bands could be detected. Ultraviolet irradiation gives the same effects as that with pure pyruvic acid.

Chlorotrimethylsilane and Styrene

The infrared spectrum of this binary mixture is shown in Figure 18. The absorption which is unique to styrene is observed at 5.95
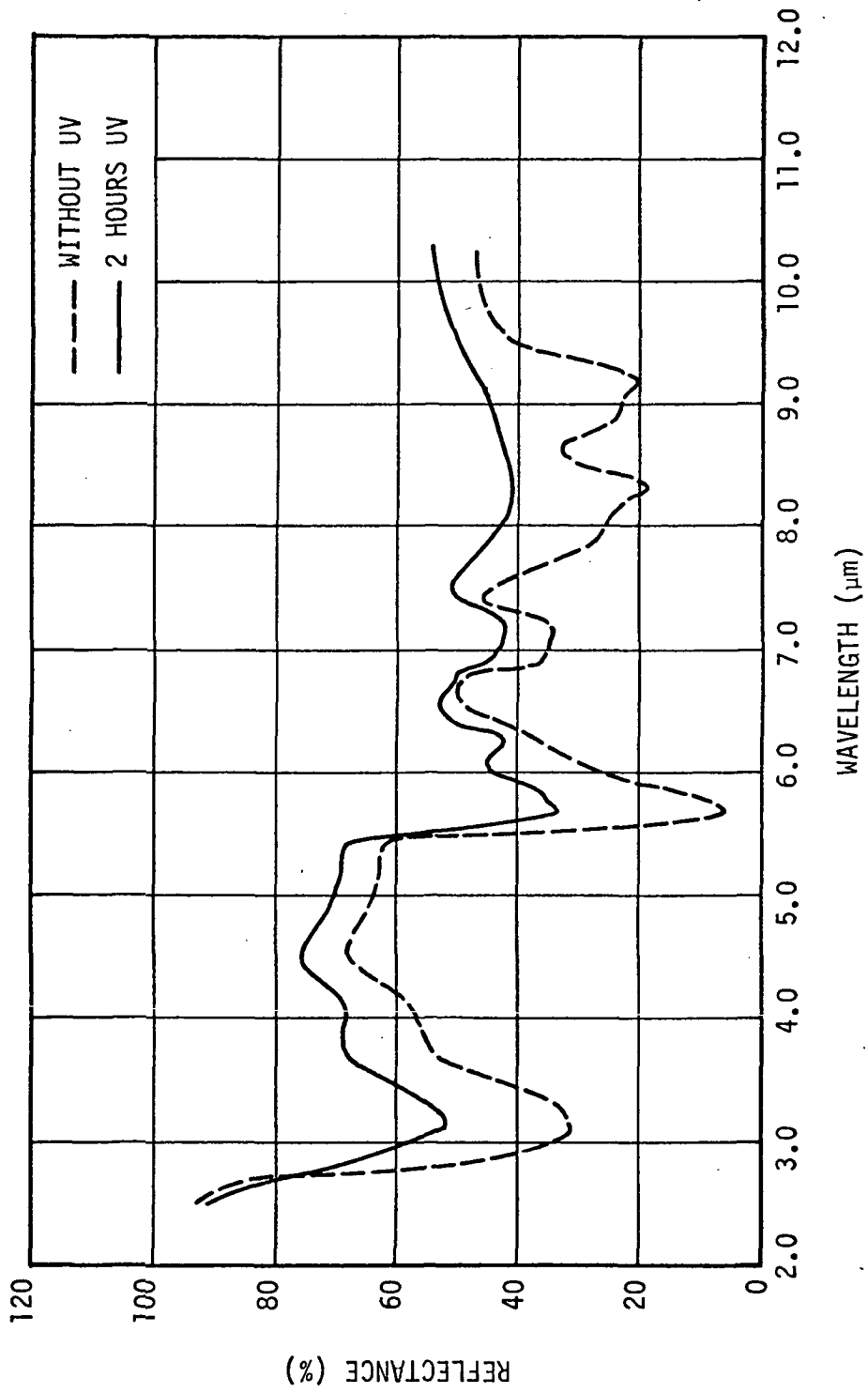
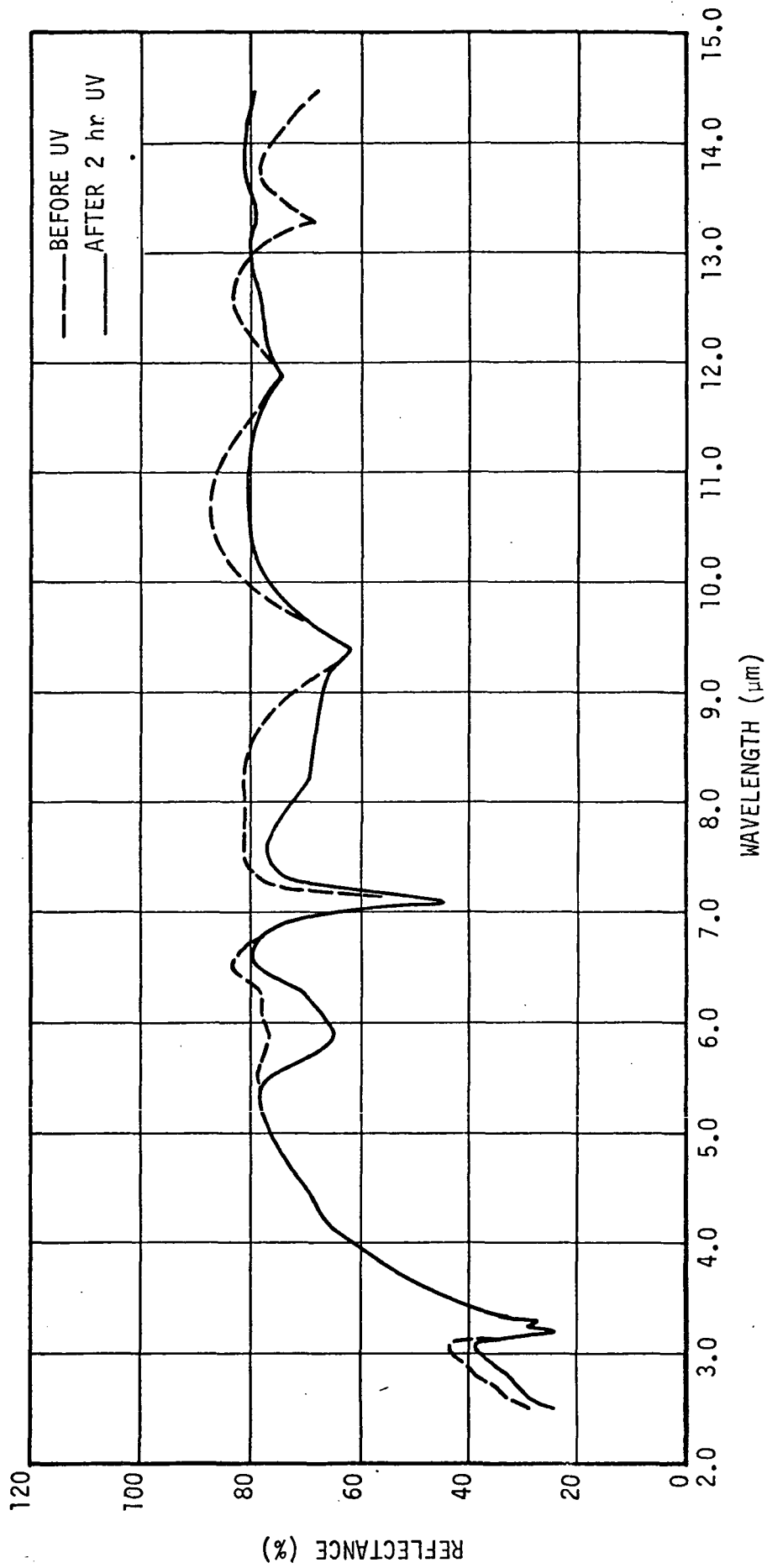FIGURE 17. SPECTRA OF PYRUVIC ACID AND WATER MIXTURE

43

FIGURE 18. SPECTRA OF CHLOROTRIMETHYLSILANE AND STYRENE MIXTURE

44

micrometers. This absorption is due to the C=C group, as mentioned before. The bands which are unique to chlorotrimethylsilane are at 7.1, 9.6, and 11.9 micrometers. The absorptions which are common to both these compounds are at 3.2 and 13.3 micrometers.

No quantitative estimation of the ratio of materials in the mixture is possible since chlorotrimethylsilane reacts with the atmosphere, as mentioned before, and is evident from the absence of the 7.98-micrometer band which is characteristic of this material (Figure 12).

This mixture turns to hard grey mass when exposed for 2 hours to ultraviolet radiation. This cannot be completely removed from the IRE surface and indicates permanent bonding.

Diethyl Adipate and Dimethyl Phthalate

The spectral response of this mixture is shown in Figure 19. There are only two absorption bands in this spectrum which are unique to diethyl adipate. These are at 7.3 and 9.7 micrometers. As mentioned before, the 7.3-micrometer band is due to CH_3 deformation and the band at 9.7 micrometers is due to C-O-C stretching vibration. The bands which are unique to dimethyl phthalate alone are at 7.8, 8.9, 9.35, and 10.45 micrometers. The bands at 7.8 and 8.9 micrometers are due to C-O stretch, and that at 9.3 micrometer is due to a disubstituted benzene ring.

For a quantitative estimation of the amount of the two components present in the mixture, the unique bands of the individual materials were considered. The 7.3-micrometer band of adipate and the 10.5-micrometer band of phthalate indicate that in the mixture they are in the ratio of approximately 1:1.
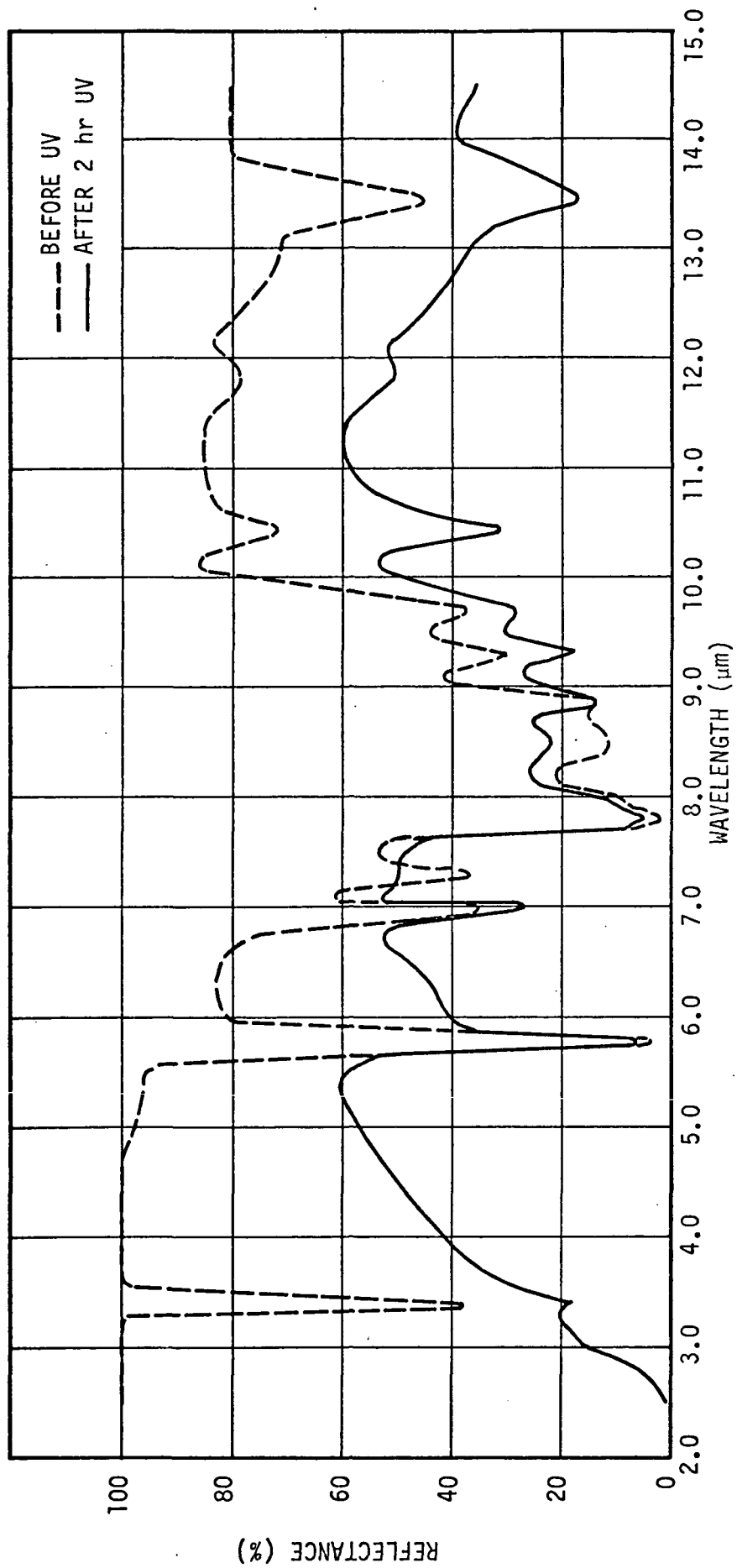
FIGURE 19. SPECTRA OF DIETHYL ADIPATE AND DIMETHYL PHTHALATE MIXTURE

Ultraviolet irradiation for 2 hours produces the same effects as that with the individual material, as can be seen from Figure 19. The new band formation in adipate around 3.0 micrometers is masked due to the strong bulk absorption of phthalate in this range of wavelength.

Methylphenyl Siloxane and Phthalate Ester

A mixture of phthalate ester and methylphenyl siloxane was studied to find out if they can be detected very easily when present in the mixture form. The spectral response is shown in Figure 20. The broad double peak between 9.0 and 10.0 micrometers immediately suggests the presence of siloxane. The absorption peak at 9.65 micrometers is due to the Si-O-Si group present in a siloxane. The absorption due to the aromatic ring present in a phthalate ester which is supposed to be around the same wavelength region is probably masked by the very strong Si-O-Si band. The peak at 9.0 micrometers is due to both the Si-O-CH_3 group of siloxane and the C-O group of phthalate ester. The two Si-CH_3 bands of siloxane are seen at 11.9 and 12.7 micrometers. The unique band of phthalate ester is clearly seen at 5.8 micrometers. This is due to C=O stretching vibration as mentioned earlier. The absorption around 7.9 micrometers due to C-O stretching vibration which is unique to phthalate ester is overlapping with the strong Si-CH_3 band of siloxane. The absorption band with two peaks observed around 3.4 micrometers is due to the C-H stretching vibration of the CH_3 group present in both siloxane and the ester. This particular group also shows absorption due to its asymmetric deformation vibration at 7.00 micrometers. Finally, the phenyl group present in the siloxane shows absorption due to the five adjacent hydrogen atoms on the ring at 13.8 micrometers, and the aromatic ring of the phthalate ester absorbs at 6.3 micrometers.
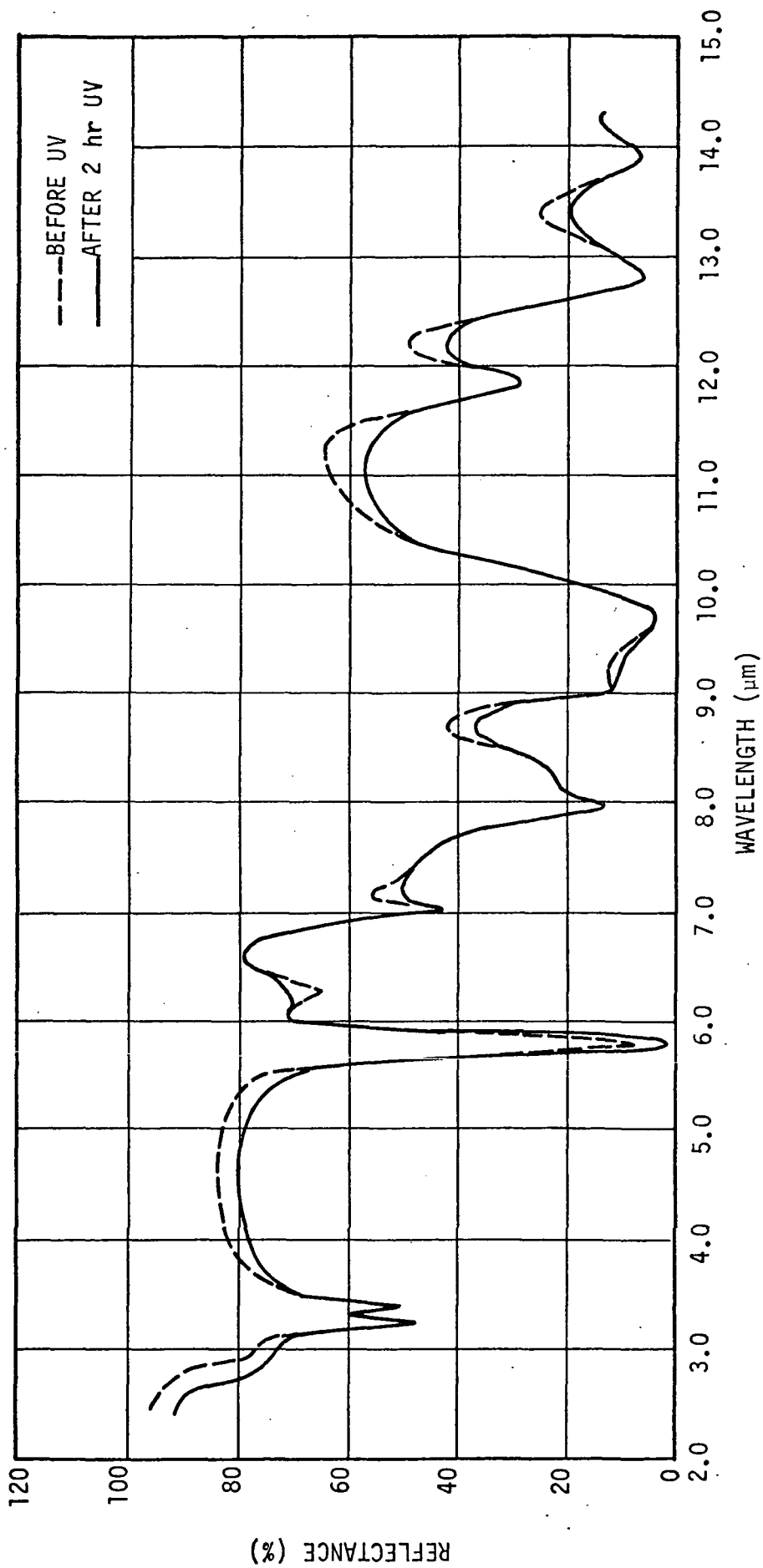
FIGURE 20. SPECTRA OF PHTHALATE ESTER AND METHYLPHENYL SILOXANE MIXTURE

48

For quantitative estimation of the amount of each component present in the mixture the absorption bands at 5.8, 9.65, 11.9, and 12.7 micrometers were considered. These bands indicate that the phthalate ester and the siloxane are in the ratio of approximately 1.5:1.

Exposure to ultraviolet radiation has the same effect as that with the individual compound. The band at 5.8 micrometers increases and a new band starts appearing around 3.0 micrometers, as shown in Figure 20. The resulting material cannot be removed completely from the IRE surface by scrubbing with organic solvents, indicating permanent bonding.

CONCLUSIONS AND RECOMMENDATIONS

CONCLUSIONS

From all these measurements it is clear that ATR spectroscopy is a very good technique for identifying spacecraft contaminants and to monitor the changes in the chemical structure of the contaminants due to solar radiation. This technique is not limited by the small amount of material available. The sensitivity is quite high even for sample quantities as low as 10^{-6} grams per square centimeter of the IRE surface.

Present measurements show that practically all the siloxanes, silanes, and esters are drastically affected by ultraviolet irradiation. In most cases they could not be removed from the optical surface by the application of organic solvents. An active cleaning technique using oxygen discharge was tried on one phthalate ester for a brief period but did not show any observable effect. The silicones can easily polymerize due to solar ultraviolet; similarly, the esters and epoxy monomers are subject to tar formation and polymerization.

This demonstrates that the effect of solar radiation on the contaminant deposited on the optical surfaces of a space experiment can be severe and cleaning of the effected optical surfaces could be very difficult.

RECOMMENDATIONS

As mentioned before, some contaminant materials could not be studied because of the difficulty of evaporation. It is suggested that in situ ATR measurements be used for contaminant identification and to monitoring the effects of ultraviolet irradiation and active cleaning. This type of measurement will ensure that no interaction between the atmosphere

and the contaminants occurs. Moreover, in situ monitoring of the effect of active cleaning will clearly predict the extent of cleaning achieved and the chemical changes in the structure of the contaminant material.

Furthermore, this technique can be very effectively used as a continuous monitoring device in space programs such as LST, etc., for in situ monitoring of the contaminants and predicting the time when a particular optical system will need cleaning.

REFERENCES

1. Born, M. and E. Wolf, "Principles of Optics", IInd Edition, MacMillan, N.Y., 1964, pp. 277

2. Harrick, N. J. and F. K. du Pre, App. Opt. 5, 1739, 1966

3. Harrick, N. J., J. Opt. Soc. Am. 55, 851, 1965

4. Hansen, W. N. and J. A. Horton, Anal. Chem. 36, 783, 1964

5. Harrick, N. J., Anal. Chem. 36, 118, 1964

APPENDIX. MINIMUM DETECTABLE FILM THICKNESS

The spectrum of a siloxane was recorded for different film thicknesses to estimate the sensitivity of the present ATR technique. This spectrum is shown in Figure 21 for film thicknesses of 175 Å, 1750 Å, and 1.75 micrometers. Both the 175 Å film and the 1750 Å film are quite adequate for identification, with little or no spectral distortion. However, the 1.75-micrometer film is too thick for this type of sensitive technique and shows total absorption from 7.00 micrometers onwards.

A theoretical calculation shows that a germanium IRE used in conjunction with a KRS-5 backing as the third medium (refer to Figure 3) should be more sensitive than using the germanium IRE alone. Experimental verification of this finding is shown in Figure 22, where the 3.4 micrometer band of a typical hydrocarbon film of approximately 20 Å thick is measured.

The results of these studies indicate that spectra of the contaminants of interest can be obtained from very thin films (approximately 20 Å) by properly orienting the IRE design to suit the need.
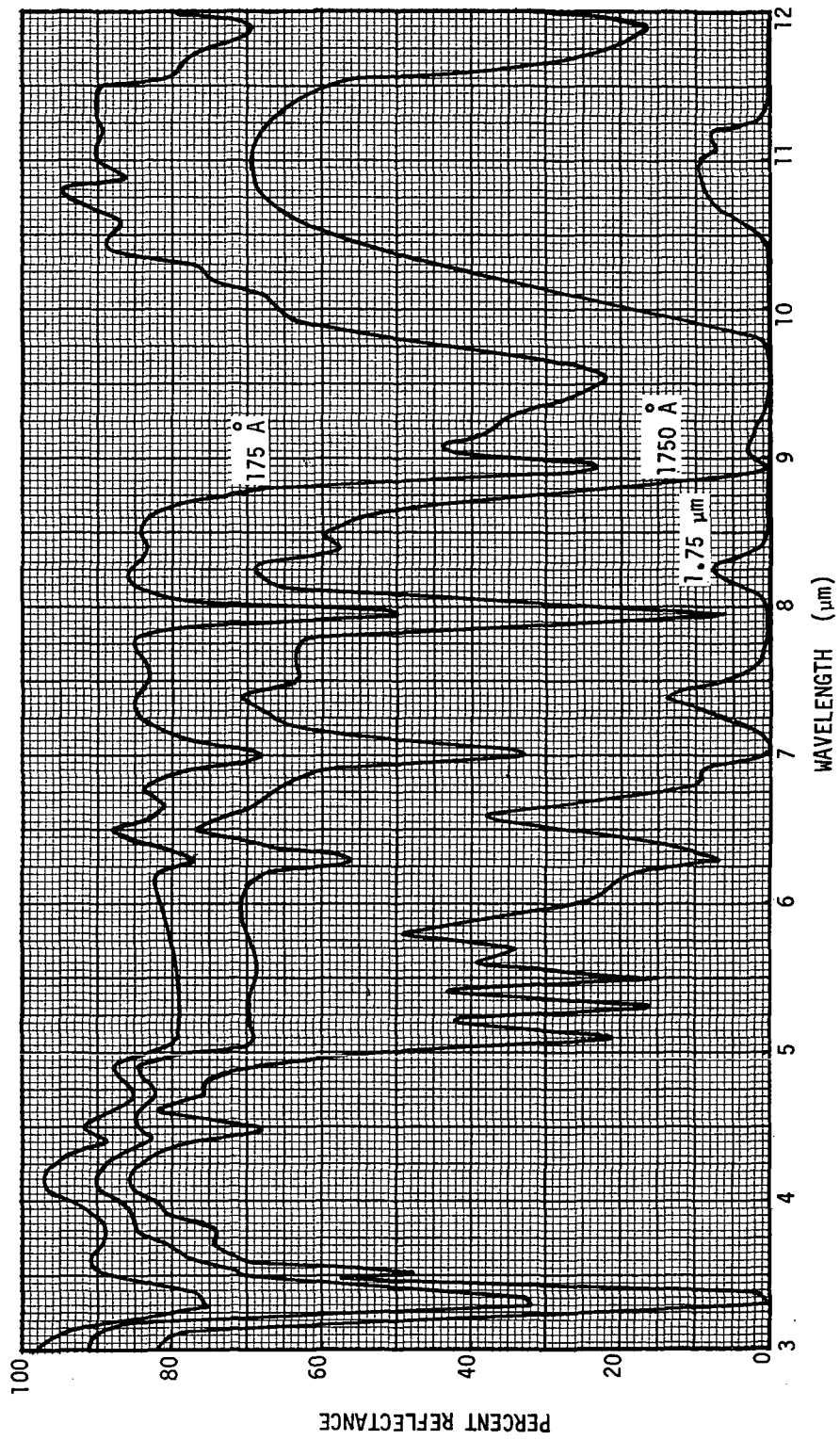
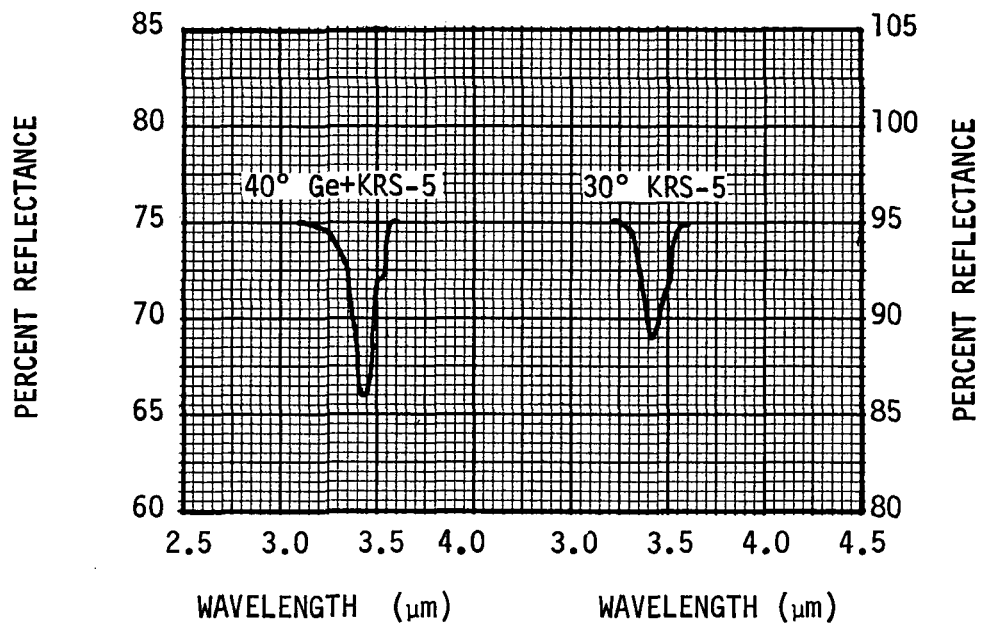FIGURE 21. THREE FILMS OF A SILOXANE ON 30-DEGREE KRS-5 IRE

54

FIGURE 22. SPECTRA OF A 3.4-MICROMETER BAND OF A HYDROCARBON
FILM APPROXIMATELY 20 Å THICK